Article

Developmental Cell

Retrograde Degenerative Signaling Mediated by the p75 Neurotrophin Receptor Requires p150^{Glued} Deacetylation by Axonal HDAC1

Graphical Abstract

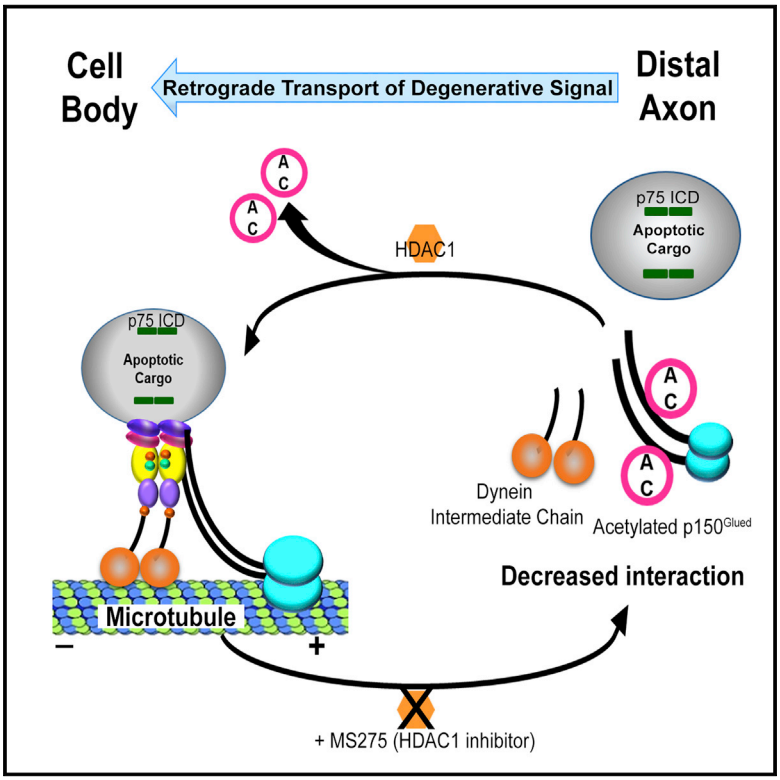

Authors

Amrita Pathak, Emily M. Stanley, F. Edward Hickman, ..., Patrizia Casaccia, Dylan T. Burnette, Bruce D. Carter

Correspondence

bruce.carter@vanderbilt.edu

In Brief

Retrograde degenerative signaling is suggested to regulate neuronal survival and degeneration. Pathak et al. identify a retrograde degenerative signal involving the intracellular domain of p75 neurotrophin receptor and histone deacetylase, HDAC1, in sympathetic neurons. HDAC1 regulates retrograde axonal transport by deacetylating dynactin subunit p150^{Glued}, enhancing its binding to dynein.

Highlights

- The intracellular domain (ICD) of p75NTR is a retrograde degenerative signal
- Trophic factor deprivation induces regulated proteolysis of p75NTR in axons
- HDAC1 is constitutively expressed in peripheral axons to regulate p75ICD transport
- HDAC1-mediated p150^{Glued} deacetylation promotes its interaction with dynein

Pathak et al., 2018, Developmental Cell *46*, 376–387
August 6, 2018
https://doi.org/10.1016/j.devcel.2018.07.001

CellPress

CellPress

Developmental Cell
Article

Retrograde Degenerative Signaling Mediated by the p75 Neurotrophin Receptor Requires p150^{Glued} Deacetylation by Axonal HDAC1

Amrita Pathak,[1,4] Emily M. Stanley,[1,4] F. Edward Hickman,[1,4] Natalie Wallace,[1] Bryson Brewer,[5] Deyu Li,[5] Shani Gluska,[6,7] Eran Perlson,[6,7] Sabine Fuhrmann,[2,3] Katerina Akassoglou,[8] Francisca Bronfman,[9] Patrizia Casaccia,[10] Dylan T. Burnette,[2] and Bruce D. Carter[1,4,11,*]

[1]Department of Biochemistry, Vanderbilt University School of Medicine, Nashville, TN, USA
[2]Department of Cell & Developmental Biology, Vanderbilt University School of Medicine, Nashville, TN, USA
[3]Department of Ophthalmology and Visual Sciences, Vanderbilt University School of Medicine, Nashville, TN, USA
[4]Vanderbilt Brain Institute, Vanderbilt University, Nashville, TN, USA
[5]Vanderbilt University School of Engineering, Nashville, TN, USA
[6]Department of Physiology and Pharmacology, Sackler Faculty of Medicine, Tel Aviv University, Tel Aviv, Israel
[7]Sagol School of Neuroscience, Tel Aviv University, Tel Aviv, Israel
[8]Gladstone Institute of Neurological Disease and Department of Neurology, University of California, San Francisco, CA, USA
[9]Center for Ageing and Regeneration (CARE UC), Faculty of Biological Sciences, Department of Physiology, Pontificia Universidad Católica de Chile, Santiago, Chile
[10]Hunter College Department of Biology, Advanced Science Research Center at The Graduate Center of the City University of New York, New York, NY, USA
[11]Lead Contact
*Correspondence: bruce.carter@vanderbilt.edu
https://doi.org/10.1016/j.devcel.2018.07.001

SUMMARY

During development, neurons undergo apoptosis if they do not receive adequate trophic support from tissues they innervate or when detrimental factors activate the p75 neurotrophin receptor (p75NTR) at their axon ends. Trophic factor deprivation (TFD) or activation of p75NTR in distal axons results in a retrograde degenerative signal. However, the nature of this signal and the regulation of its transport are poorly understood. Here, we identify p75NTR intracellular domain (ICD) and histone deacetylase 1 (HDAC1) as part of a retrograde pro-apoptotic signal generated in response to TFD or ligand binding to p75NTR in sympathetic neurons. We report an unconventional function of HDAC1 in retrograde transport of a degenerative signal and its constitutive presence in sympathetic axons. HDAC1 deacetylates dynactin subunit p150^{Glued}, which enhances its interaction with dynein. These findings define p75NTR ICD as a retrograde degenerative signal and reveal p150^{Glued} deacetylation as a unique mechanism regulating axonal transport.

INTRODUCTION

Neuronal apoptosis is necessary for vertebrate development and establishment of proper neural circuitry. However, abnormal apoptosis is the basis for many neuropathologies, highlighting the need to define the mechanisms by which it is regulated in order to develop new therapies. The balance between neuronal survival and degeneration in the peripheral nervous system is mostly governed by the availability of neurotrophic factors, including the neurotrophins. The neurotrophins mediate survival and differentiation through binding to the tropomyosin receptor kinase (Trk) family of tyrosine kinase receptors (Deinhardt and Chao, 2014). All neurotrophins can also bind to the p75 neurotrophin receptor (p75NTR), a member of the tumor necrosis factor (TNF) receptor superfamily, which may elicit distinct effects, including the induction of apoptosis and axonal degeneration, depending on the cellular context (Ceni et al., 2014; Kraemer et al., 2014; Vicario et al., 2015).

Neurotrophins are produced by the target tissues innervated by developing neurons; thus, these factors act locally on axon ends and generate signals that must be conveyed back to the cell body. The mechanisms of retrograde survival signaling have been extensively studied, primarily in sympathetic and sensory neurons that depend on nerve growth factor (NGF) for survival (Harrington and Ginty, 2013; Scott-Solomon and Kuruvilla, 2018; Wu et al., 2009). Loss of trophic factor input leads to a reduction in pro-survival signals reaching the soma. However, there is growing evidence that trophic factor deprivation (TFD) also results in pro-apoptotic signaling that starts at the periphery and is sent back to the cell body (Ghosh et al., 2011; Mok et al., 2009; Simon et al., 2016). When NGF was selectively withdrawn from distal axons of sympathetic neurons, there was an increase in phosphorylation of c-Jun in the cell bodies. This increase was blocked when the axons were treated with the microtubule-disrupting agent colchicine, suggesting the existence of a retrograde transport-dependent apoptotic mechanism (Mok et al., 2009). Blocking axonal activation of the stress-induced dual leucine zipper kinase (DLK) or c-Jun N-terminal kinase (JNK) also prevented sensory neuron apoptosis following TFD (Simon

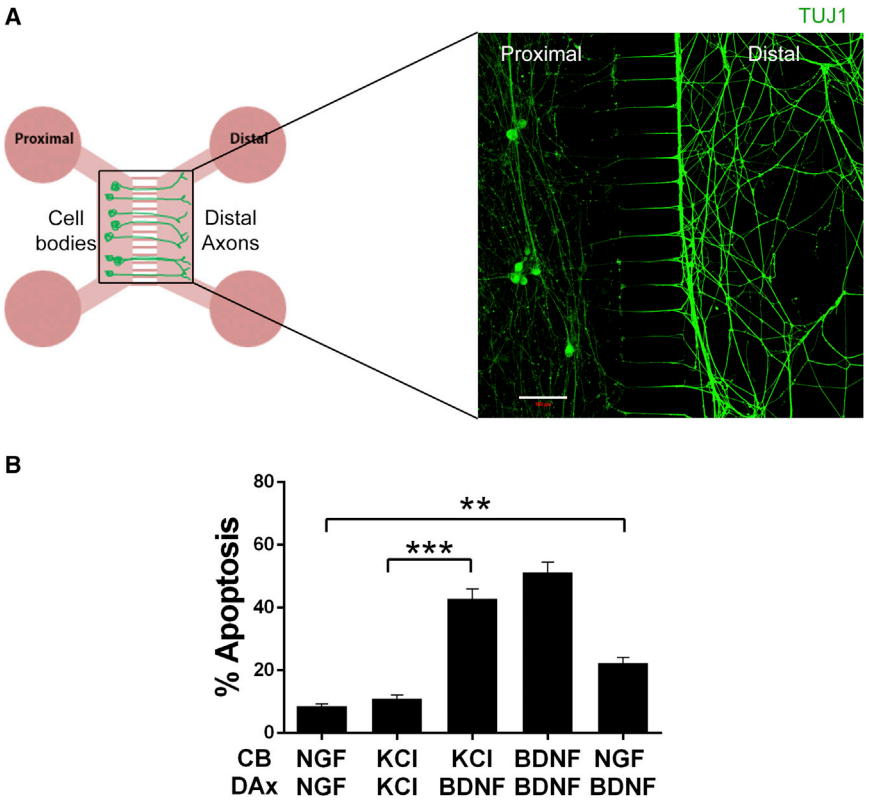

Figure 1. Retrograde Apoptotic Signaling by BDNF in Sympathetic Neurons

(A) Schematic representation of microfluidic chamber culture system and representative image of sympathetic neurons immunostained with TUJ1 (green). Scale bar represents 100 μm.

(B) Activation of p75NTR in distal axons (DAx) results in apoptosis at the cell soma. After the axons reached the distal sides, NGF was removed, and the cell bodies (CB) and DAx were treated with 12.5 mM KCl or NGF, with or without 200 ng/mL BDNF for 48 hr, as indicated. The bar on the extreme left of the graph represents neurons maintained in 20 ng/mL NGF on the CB and DAx, while for the extreme right bar, axons were treated with 200 ng/mL BDNF, and CB were given 2 ng/mL NGF. After 48 hr of treatment, the neurons were fixed and stained for TUJ1 and DAPI, and pyknotic nuclei were quantified as a measure of apoptosis. Depicted are the means ± SEM for n = 5; **, $p < 0.01$; ***, $p < 0.001$; 2-way ANOVA with a Tukey's multiple comparisons test.

et al., 2016). However, the molecular components of this retrograde signaling are yet to be defined.

Activation of p75NTR has also been implicated in apoptosis following TFD; for example, sympathetic neurons from $p75^{-/-}$ mice are resistant to NGF withdrawal (Majdan et al., 2001; Nikoletopoulou et al., 2010). How the receptor contributed to the induction of apoptosis was not determined. However, it is notable that direct activation of p75NTR by ligand binding at distal axons can trigger neuronal apoptosis (Tauris et al., 2011; Taylor et al., 2012; Yano et al., 2009), suggesting that there may be a shared mechanism with TFD. Many of p75NTR's downstream signals, including the activation of cell death pathways, require regulated proteolysis of the receptor by α-secretase and the γ-secretase complex to release the intracellular domain (ICD) (Skeldal et al., 2012). Therefore, we hypothesized that the p75NTR ICD may be a key component of the retrograde degenerative signal following TFD or p75NTR activation by ligand binding.

Retrograde axonal transport is driven by the microtubule minus-end-directed motor protein dynein, which consists of a dimer of heavy chains and additional intermediate and light chains. Dynein associates with the activator complex dynactin, which is composed of more than 20 proteins, including the largest subunit $p150^{Glued}$. A dimer of $p150^{Glued}$ binds to the dynein intermediate chain (DIC) through its coiled-coil domain (CC1) and is required for processivity of the complex (Karki and Holzbaur, 1995; King and Schroer, 2000; McKenney et al., 2014). Formation of this complex and how it is regulated is still an active area of investigation.

Surprisingly, several histone deacetylases (HDACs) have recently been shown to influence axonal transport. While best characterized for their role in regulating gene expression, several HDACs can shuttle out of the nucleus and modify other targets (Cho and Cavalli, 2014). Histone deacetylase 1 (HDAC1) was recently shown to translocate from the nucleus into the axons of cortical and hippocampal neurons following TNF and glutamate treatment, where it associated with kinesins. This association disrupted mitochondrial transport, which led to axon degeneration (Kim et al., 2010).

Here, we reveal a role for HDAC1 in retrograde degenerative signaling through regulating the formation of the dynactin-dynein complex. We further identify the ICD of p75NTR as a retrograde pro-apoptotic signal triggered by p75NTR activation due to ligand binding or TFD in sympathetic neurons.

RESULTS

Retrograde Apoptotic Signaling Requires Localized Cleavage of p75NTR

To investigate the mechanisms of retrograde degenerative signaling, sympathetic neurons from rat superior cervical ganglia were cultured in microfluidic chambers, which allow separation of the cell bodies from the distal axons (Figure 1A), thus mimicking the different environmental milieu for distal axons and cell bodies *in vivo*. Since NGF binds to a complex of p75NTR and TrkA (Hempstead et al., 1991), which would complicate the analysis of activating p75NTR alone, NGF was removed and neurons were kept alive in KCl. To selectively stimulate p75NTR, brain-derived neurotrophic factor (BDNF) was used, since it has been implicated as an endogenous pro-apoptotic ligand for p75NTR in this system (Deppmann et al., 2008). BDNF or NGF was then added to the distal axons or cell bodies, as indicated. There was a significant increase in cell death in response to BDNF treatment of axons (Figure 1B), even if the cell bodies received limited trophic support from 2 ng/mL NGF.

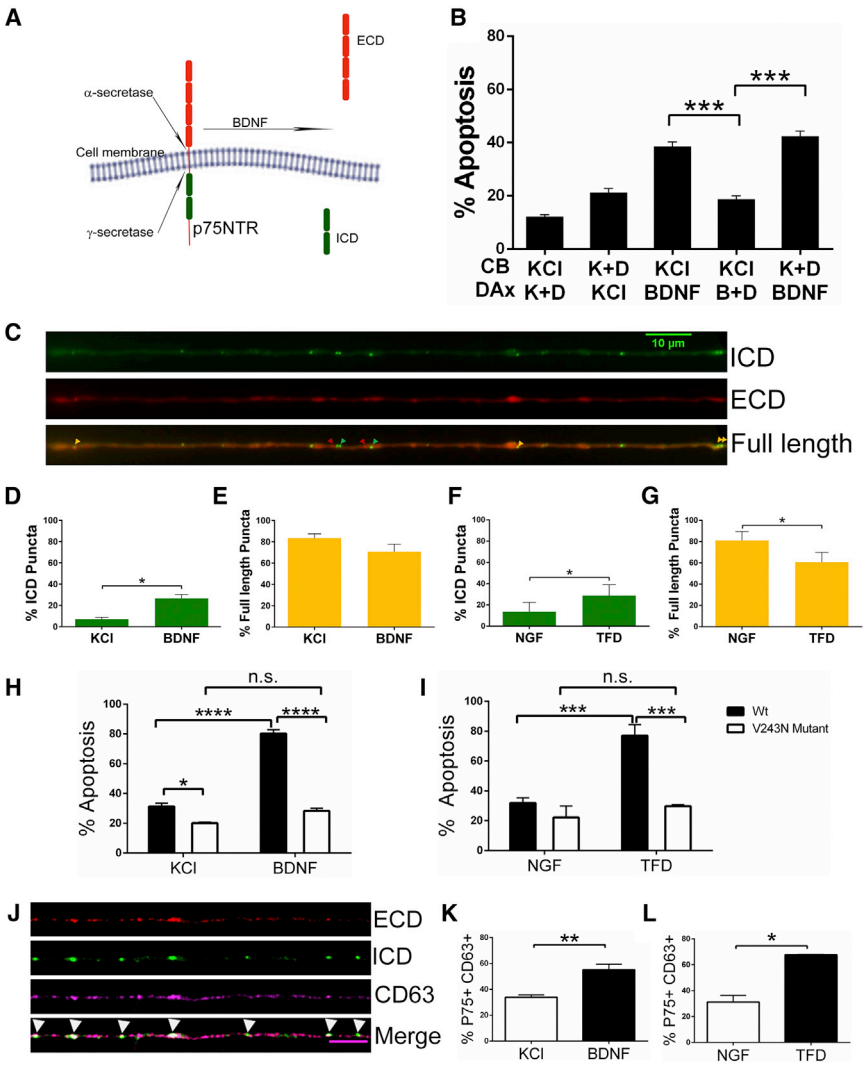

Figure 2. P75NTR Cleavage in Distal Axons Is Necessary for Apoptosis

(A) Schematic showing the cleavage of p75NTR.

(B) Inhibition of axonal γ-secretase prevents p75NTR-mediated apoptosis. Sympathetic neurons were cultured in microfluidic chambers, and cell bodies (CB) and distal axons (DAx) were treated with 12.5 mM KCl (K) or 200 ng/mL BDNF (B) ± the γ-secretase inhibitor, 250 nM DAPT (D), for 48 hr, as indicated. The bars depict the means ± SEM for n = 3–5; ***, $p < 0.001$, Student's t test with Welch correction among indicated groups. See also Figure S1.

(C) Representative image of mCherry-p75NTR-GFP in sympathetic neurons showing full-length p75NTR (yellow arrowheads), the released ECD (red arrowheads), and the liberated ICD (green arrowheads) in axons (scale bar = 10 μM). See also Figure S1.

(D and E) Quantification of the number of p75NTR ICD only (green) and full-length p75NTR (yellow) puncta in axons after treatment with KCl (control) or BDNF for 2 hr. Depicted are the means ± SEM from at least 3 different experiments (KCl, n = 266 and BDNF, n = 255 events); *, $p < 0.05$, Student's t test.

(F and G) Quantification of the number of p75NTR ICD only (green) and full-length p75NTR (yellow) puncta under control conditions and after trophic factor deprivation (TFD) for 14 hr. Depicted are the means ± SEM from 3 different experiments (NGF, n = 212 and TFD, n = 383 events); *, $p < 0.05$, Student's t test.

(H and I) Expression of cleavage-resistant V243N mutant p75NTR prevents neuronal apoptosis induced by BDNF or TFD. Sympathetic neurons were electroporated with either wild-type or V243N mutant mCherry-p75NTR-GFP and cultured in NGF. The neurons were then treated with KCl +/- 200 ng/mL BDNF, maintained in 20 ng/mL NGF or NGF was removed, as indicated for 48 hr. The bars depict the means ± SEM for n = 3–5; *, $p < 0.05$, ***, $p < 0.001$, ****, $p < 0.0001$; 2-way ANOVA with a Sidak and Tukey's multiple comparisons test among indicated groups. See also Figure S1.

(J) Visualization of p75NTR in CD63-labeled MVBs. Neurons electroporated with mCherry-p75NTR-GFP and stained for endogenous CD63 (magenta). P75NTR-ECD shown in red and P75NTR-ICD in green. Scale bar represents 5 μm.

(K and L) Quantification of P75NTR and CD63 double-labeled puncta after the neurons were treated with KCl +/- 200 ng/mL BDNF for 2 hr (K), or maintained in 20 ng/mL NGF or NGF was removed for 14 hr (L). The bars depict the means ± SEM for n = 3–5; *, $p < 0.05$; **, $p < 0.01$, Student's t test with Welch correction among indicated groups.

These results support the hypothesis that p75NTR activation in axons can trigger a retrograde degenerative signal.

Proteolytic cleavage of p75NTR by α- and γ-secretase releases its ICD (Figure 2A) as well as a number of associated signaling components, which traffic to the nucleus to mediate apoptosis (Kraemer et al., 2014). Since activation of p75NTR on the distal axons induced cell death back in the soma, we hypothesized that the receptor was locally cleaved in the axons and that this proteolysis was required to generate the retrograde apoptotic signal. To test this hypothesis, we added BDNF to the distal axons along with the γ-secretase inhibitor N-[N-(3,5-Difluorophenacetyl)-L-alanyl]-S-phenylglycine t-butyl ester (DAPT) and compared the subsequent cell death to that induced in the presence of DAPT exclusively on the cell somas. When present in the distal axons, DAPT completely abrogated apoptosis. However, when the γ-secretase inhibitor was applied only to the cell somas and BDNF to the distal axons, there was no protective effect (Figure 2B). These data suggest that activation of p75NTR induces local receptor proteolysis, which is necessary for retrograde apoptotic signaling (Figures 2B, S1A, and S1B).

To directly assess axonal p75NTR cleavage in response to a pro-apoptotic ligand, we electroporated a dual-tagged p75NTR reporter construct into the neurons, which has mCherry on the N-terminus and green fluorescent protein (GFP) on the C-terminus. The expression of the construct was detected throughout the neuron, including in the axons (Figure S1C). This mCherry-p75NTR-GFP reporter was previously utilized to

investigate the localization of the cleaved receptor products in astrocytes and can differentiate between uncleaved, full-length p75NTR (yellow), cleaved p75NTR ICD (green), and extracellular domain (ECD) (red) (Schachtrup et al., 2015). After electroporation, the neurons were allowed to recover in NGF, then switched to KCl with or without BDNF for 2 hr, and the number of mCherry, GFP, or overlapping puncta in the axons was quantified. The mCherry signal was found to be very weak, making quantification difficult; therefore, to avoid underestimating the amount of ECD, we preincubated live neurons with an antibody to the ECD that does not interfere with ligand binding. This antibody was tagged with ATTO-550 to enhance the mCherry signal of ECD (hereafter referred to as "mCherry"). Puncta positive for both GFP and mCherry (yellow, Figure 2C) were considered to be full-length receptors, although we cannot rule out the possibility that p75NTR was cleaved and both the ICD and ECD remained localized and too close to be resolved. Puncta that were only GFP+ or mCherry+ were considered as independent ICD and ECD, respectively. BDNF significantly increased the number of GFP+ only (ICD) puncta, suggesting p75NTR cleavage within the axons (Figure 2D). The majority of puncta were labeled with both mCherry and GFP, and BDNF treatment did not induce a significant change in the number of full-length receptors, suggesting only a small fraction of p75NTR undergoes cleavage after BDNF treatment (Figure 2E). Similar results were reported using western blot to detect p75NTR cleavage: only a fraction of the receptor is cleaved and the majority remains full length (Jung et al., 2003; Kanning et al., 2003; Kenchappa et al., 2006). We also detected a very small percentage of mCherry+ only puncta, reflecting the ECD, which was not altered by BDNF (data not shown). We interpret the low number of ECD fragments as a majority being lost due to most of the ECD having been released by α-secretase at the plasma membrane.

Since TFD also initiates a retrograde degenerative signal (Ghosh et al., 2011; Mok et al., 2009; Simon et al., 2016), we investigated the possibility that NGF withdrawal could stimulate local p75NTR proteolysis. NGF was withdrawn and the axons were live- imaged after 14 hr, which we reasoned would be long enough to induce p75NTR cleavage, but prior to the neurons committing to apoptosis (Deckwerth and Johnson, 1993). There was a significant decrease in full-length receptor after NGF withdrawal and a corresponding increase in the fraction of GFP+ only puncta (Figures 2F and 2G), indicating that TFD can induce the cleavage of p75NTR in axons.

Although treatment of the axons with DAPT blocked neuronal death (Figure 2B), DAPT inhibits the cleavage of all γ-secretase substrates. Therefore, we investigated whether the cleavage of p75NTR specifically was necessary for the apoptotic signal. We generated a Val243Asn (V243N) mutation in the extracellular juxtamembrane region of the mCherry-p75NTR-GFP construct, which introduces a glycosylation site that prevents the receptor from undergoing proteolysis and blocks p75NTR-mediated apoptosis (Underwood et al., 2008). We confirmed that the V243N mutant did not undergo proteolysis (Figures S1D and S1E). Importantly, when this construct was expressed in the neurons, it prevented cell death induced by BDNF or by NGF withdrawal (Figures 2H and 2I). Since both α- and γ-secretase cleavages were inhibited by the expression of the V243N construct, these results do not distinguish between the ICD produced by γ-secretase and the carboxy-terminal fragment produced by α-secretase as the essential death signal. However, these findings indicate that cleavage specifically of p75NTR is required for apoptotic signaling generated by BDNF binding to p75NTR or by NGF withdrawal.

The cleavage of p75NTR in axons raised the question as to how the ICD would be transported back to the soma. It was recently reported that p75NTR is present in CD63+ multi-vesicular bodies (MVBs) in sympathetic neuron cell bodies after BDNF treatment (Escudero et al., 2014) and MVBs have been implicated in retrograde NGF-TrkA signaling (Ye et al., 2018). Therefore, we hypothesized that p75NTR ICD may also be transported in MVBs. In neurons electroporated with the mCherry-p75NTR-GFP reporter, we found a significant increase in the co-localization of GFP signal with CD63+ immunostaining in the axons following BDNF stimulation or NGF deprivation (Figures 2J–2L). These results suggest that MVBs transport the p75NTR apoptotic signal from axons to the neuronal soma.

Axonal HDAC1 Is Required for Retrograde Degenerative Signaling

Recent studies have revealed a role for several HDACs in regulating axonal transport (Cho and Cavalli, 2014). Therefore, we hypothesized that HDACs may also be involved in retrograde degenerative signaling. Addition of the general class I HDAC inhibitor sodium butyrate selectively to distal axons along with BDNF blocked neuronal death (Figure S2A). Since sodium butyrate is rather non-selective, we tested the effects of MS275, which preferentially inhibits HDAC1 (Bertrand, 2010; Hu et al., 2003). Treatment of the axons with MS275 completely prevented p75NTR-mediated retrograde apoptotic signaling (Figure 3A). Importantly, the addition of MS275 to the cell bodies had no effect on the apoptosis induced by BDNF in the distal axons, indicating that nuclear HDAC1 activity is not required for apoptosis. To confirm the specificity for HDAC1, we knocked down the deacetylase with a short hairpin RNA (shRNA)-expressing lentivirus (Figure 3B) that selectively silences HDAC1 without affecting the other HDACs (Kim et al., 2010). After confirming the knockdown (Figure 3B), we found that the apoptosis induced by axonal BDNF was completely prevented (Figure 3C), further supporting an essential role for HDAC1 in this retrograde degenerative signaling.

Since HDAC6 is a well-established regulator of axonal transport through deacetylation of tubulin (d'Ydewalle et al., 2011), we also evaluated the effects of Tubastatin A, an HDAC6-selective inhibitor. Addition of Tubastatin A to the distal axons did not affect BDNF-induced apoptosis, indicating that HDAC6 activity is not required (Figure 3D).

Class I HDACs, including HDAC1, primarily localize to the nucleus (Cho and Cavalli, 2014; Haberland et al., 2009); however, it was recently reported that HDAC1 can translocate into axons following injury (Kim et al., 2010). Since the sympathetic neurons used here were not subjected to any insult prior to p75NTR activation, our results suggested that HDAC1 is constitutively present in these axons. By immunostaining, we analyzed HDAC1 expression in the presence of NGF, which promotes robust survival of these neurons and found HDAC1 expression in the axons as well as the nucleus (Figure 3B). The specificity of the staining was confirmed by HDAC1 knockdown. We also isolated pure axons from the neurons and fractionated the cell bodies into

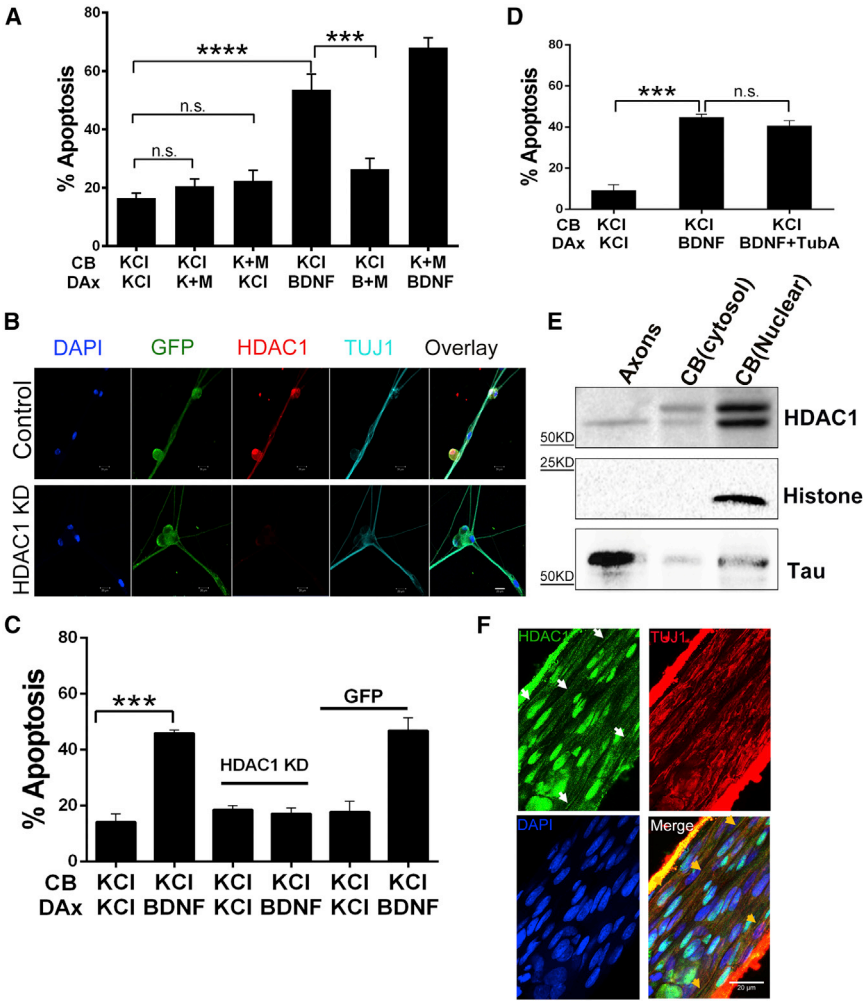

Figure 3. Axonal HDAC1 Is Required for p75NTR-Mediated Retrograde Apoptotic Signaling

(A) Inhibition of axonal HDAC1 blocks p75NTR-mediated neuronal apoptosis. Sympathetic neurons were cultured in microfluidic chambers, and cell bodies (CB) and distal axons (DAx) were treated with 12.5 mM KCl or 200 ng/mL BDNF +/- 5 μm MS275 (M) for 48 hr, as indicated. Depicted are the means ± SEM for n = 3–4; ***, p < 0.001; ****, p < 0.0001; 2-way ANOVA with a Tukey's multiple comparisons test.

(B) Representative images of sympathetic neurons infected with a lentivirus expressing HDAC1 knockdown shRNA and co-expressing GFP (green) or a GFP expressing control lentivirus. The neurons were immunostained for HDAC1 (red) and TUJ1 (teal). DAPI was used to label the nuclei. Scale bar represents 20 μm.

(C) Silencing HDAC1 prevents p75NTR-mediated neuronal apoptosis. Sympathetic neurons with HDAC1 knocked down or expressing a GFP control were treated on their CB and DAx with 12.5 mM KCl or 200 ng/mL BDNF, for 48 hr as indicated. Depicted are the means ± SEM for n = 3–4; ***, p < 0.001; 2-way ANOVA with a Tukey's multiple comparisons test.

(D) Inhibition of HDAC6 did not affect p75NTR-induced apoptosis. Neurons were treated on their CB and DAx with 12.5 mM KCl, 200 ng/mL BDNF, or 200 ng/mL BDNF + 5 μm Tubastatin A (TubA), as indicated. Depicted are the means ± SEM for n = 3–4; ***, p < 0.001; n.s., not significant; 2-way ANOVA with a Tukey's multiple comparisons test.

(E) Axons and CB were collected from sympathetic neurons, and lysates were western blotted for HDAC1 and Histone H3 or Tau to confirm the purity of nuclear and axonal fractions, respectively.

(F) HDAC1 is constitutively expressed in sympathetic axons *in vivo*. Nerve fibers descending proximal to the superior cervical ganglia were isolated from P4–5 rats, fixed and immunostained for HDAC1 and TUJ1. White arrows indicate the HDAC1-stained axons, and yellow arrowheads indicate the same axons showing TUJ1 co-staining (scale bar = 20 μM).

cytosolic and nuclear fractions, and then the 3 compartments were immunoblotted for HDAC1. A single band of 66 kDa for HDAC1 was detected in the axons, whereas a doublet was present in the cytosolic and nuclear fractions (Figure 3E). This doublet is consistent with the phosphorylation of HDAC1 that was recently reported to maintain its localization in the nucleus (Zhu et al., 2017). Finally, to confirm that HDAC1 is present in sympathetic axons *in vivo* and not just in cultured neurons, we isolated the descending nerve proximal to the superior cervical ganglia from post-natal day (P)4–5 rats and immunostained for the deacetylase. HDAC1 was detectable in axon fibers of the nerve (as well as in glial nuclei), indicating that it is constitutively expressed in peripheral axons (Figure 3F). The specificity of the signal in the nerve fibers was confirmed by staining brain tissue, where only nuclei were detected (Figure S2B).

HDAC1 Is Required for Retrograde Axonal Transport of the p75NTR Intracellular Domain

As a first step in retrograde trafficking, p75NTR is internalized through a mechanism requiring the GTPase dynamin (Deinhardt et al., 2007; Hibbert et al., 2006), which can be blocked by the inhibitor Dynasore (Kirchhausen et al., 2008; Macia et al., 2006; Escudero et al, 2014). We also observed p75NTR internalization following BDNF treatment (Figures 4A and 4B), which was necessary for retrograde apoptotic signaling, since the addition of Dynasore along with BDNF in the distal axons prevented neuronal cell death (Figure 4C). However, there was no significant effect of MS275 on receptor internalization (Figures 4A and 4B), indicating that HDAC1 activity is not required for p75NTR endocytosis.

Because inhibition of HDAC1 did not affect p75NTR internalization, we hypothesized that the deacetylase was required for retrograde trafficking of the receptor. To investigate p75NTR axonal transport, we used the mCherry-p75-GFP reporter, which allowed us to track both the full-length receptor and the liberated ICD. The neurons were treated with BDNF in the presence or absence of MS275 for 2 hr and live-imaged to assess the movement of the cleaved ICD and the full-length p75NTR (Figures 5A and 5B). The ATTO-550 labeled antibody to the ECD of p75NTR was included to enhance detection of the ECD fragment. Following BDNF treatment, there was a significant increase in

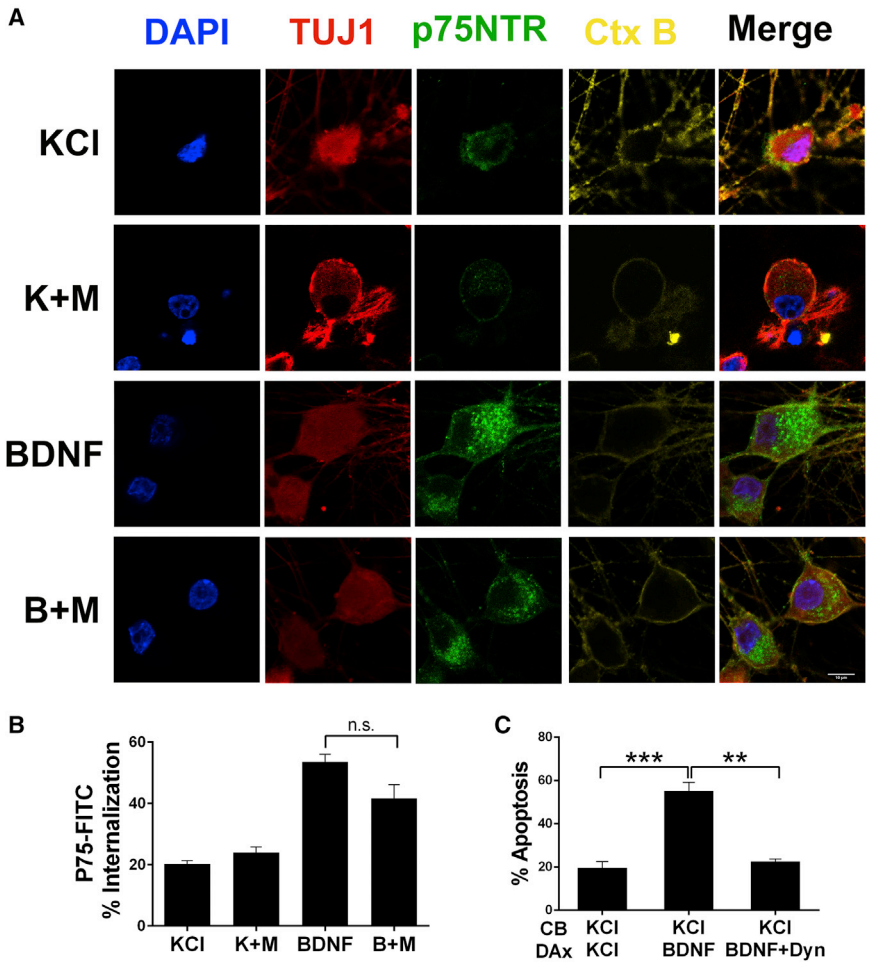

Figure 4. HDAC1 Does Not Affect p75NTR Internalization, which Is Necessary for Neuronal Apoptosis

(A) Representative images of p75NTR immunoendocytosis in the presence or absence of BDNF ± MS275. Sympathetic neurons were incubated with an antibody to p75NTR ECD conjugated to FITC at 4°C then treated for 4 hr with 12.5 mM KCl or 200 ng/mL BDNF ± 5 μm MS275 (M) at 37°C, as indicated, and then fixed and immunostained for TUJ1 (red). P75NTR is shown in green, and nuclei are labeled with DAPI (blue). Cholera toxin B (Ctx B) was used to define the plasma membrane (yellow). Scale bar represents 10 μm.

(B) Quantification of p75NTR internalization following BDNF (B) treatment ± MS275 (M). The relative amount of internalized fluorescence corresponds to the intracellular fluorescence normalized to the cell surface associated fluorescence in complete z stacks of confocal images. Shown is the average internalized fluorescence ± SEM for n = 3 (70 neurons); n.s., not significant; Student's t test with Welch correction.

(C) Internalization of p75NTR is necessary for neuronal apoptosis. Neurons were cultured in microfluidic chambers, and cell bodies (CB) and distal axons (DAx) were treated with 12.5 mM KCl or 200 ng/mL BDNF ± 80 μm Dynasore (Dyn) for 48 hr, as indicated. Depicted are the means ± SEM for n = 4; **, $p < 0.01$; ***, $p < 0.001$; 2-way ANOVA with Tukey's multiple comparisons test.

the number of ICD-only, GFP+ particles moving retrogradely; however, this increase was completely blocked by addition of MS275, indicating that HDAC1 activity is required for the BDNF-induced retrograde movement (Figure 5C). BDNF also increased the instantaneous velocity of the GFP+ puncta moving in a retrograde direction; however, this was not notably affected by inhibition of HDAC1 (Figure S3).

Interestingly, the percentage of full-length p75NTR, or co-localized ECD and ICD, particles moving retrogradely also increased after BDNF treatment, and MS275 prevented this increase (Figure 5D). There was also an increase in the instantaneous velocity of full-length p75NTR moving in the retrograde direction after BDNF treatment, but MS275 had little effect. Although we cannot rule out the possibility that full-length particles containing both the ECD and the ICD contribute to the subsequent cell death, the fact that inhibiting receptor cleavage in the distal axons prevented apoptosis (Figure 2B) suggests that it is the retrograde transport of the liberated ICD that is the determining factor for the fate of the neuron.

Based on the requirement for p75NTR in the apoptosis of sympathetic neurons following NGF withdrawal (Majdan et al., 2001; Nikoletopoulou et al., 2010) and the induction of p75NTR cleavage by TFD (Figures 2F and 2G), we hypothesized that loss of NGF signaling would also induce retrograde trafficking of the p75NTR ICD and that this transport would also require HDAC1 activity. We found a significant increase in the number of p75NTR ICD, GFP+ particles moving in the retrograde direction following NGF withdrawal, and this retrograde transport was blocked by HDAC1 inhibition (Figure 5E). Retrograde transport of full-length p75NTR, or closely localized ICD and ECD, was also increased following NGF removal, and this was also blocked by MS275 (Figure 5F). Similar to p75NTR activation by BDNF binding, the instantaneous velocity of the retrogradely moving p75 was increased after NGF withdrawal, but there was no marked effect of MS275. Taken together, the live imaging data indicate that HDAC1 activity is required for retrograde transport of the p75NTR ICD, which mediates a degeneration signal.

HDAC1 Deacetylates the p150^{Glued} Subunit of Dynactin

To determine the relevant substrates of HDAC1 in the axons, neurons were grown on transwell inserts in the presence of NGF and MS275 to maximize the acetylation of HDAC1 substrates, and axons were collected. Trypsin-digested axonal proteins were immunoprecipitated with anti-acetyl lysine and analyzed by mass spectrometry. A total of 100 axonal proteins potentially harboring lysine-acetylation were identified; among these, one candidate that caught our attention was dynactin1/p150^{Glued}. The p150^{Glued} subunit is the major polypeptide of the dynactin complex and is necessary for the processivity of the dynein motor (King and Schroer, 2000; McKenney et al., 2014). We validated the lysine-acetylation site on p150^{Glued} by

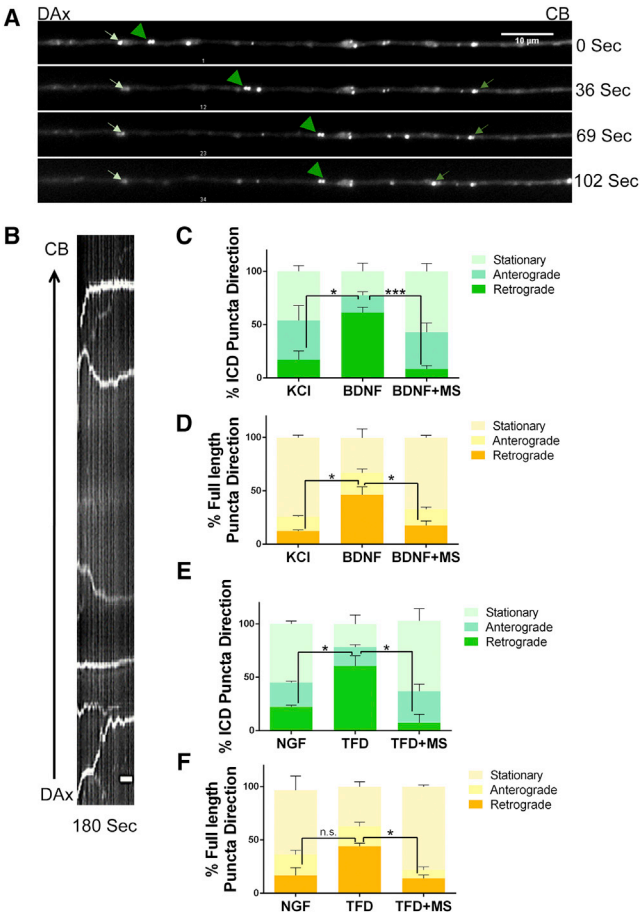

Figure 5. HDAC1 Is Required for Retrograde Axonal Transport of p75NTR Intracellular Domain

(A) Representative images of an axon from a neuron treated with BDNF. Frames were collected from a time-lapse movie showing p75NTR ICD particles moving in the retrograde (green arrowheads) or anterograde (green arrows) direction or stationary (white arrows). Scale bar represents 10 μm.

(B) Kymograph generated from time-lapse images displaying the trajectory of p75NTR ICD. Scale bar represents 1 μm.

(C–F) Quantification of moving and stationary p75NTR ICD and full-length receptor and directionality of traffic under the indicated conditions. p75NTR ICD is displayed by green stacked bar graphs, while the movement of full-length p75NTR is shown by bar graphs in different shades of yellow. Data pooled from n = 3 (means ± SEM are shown); Student's t test with Welch correction revealed that for retrograde movement of the ICD, KCl vs. BNDF, $p < 0.05$; BDNF vs. BDNF+MS, $p < 0.001$; NGF vs. TFD, $p < 0.05$; TFD vs. TFD+MS, $p < 0.05$; and for the full-length p75NTR, KCl vs. BDNF, p, 0.05; BDNF vs. BDNF+MS, p, 0.05; NGF vs. TFD, n.s.; TFD vs. TFD+MS, $p < 0.01$. See also Figure S2.

manual inspection of the spectra (Figure 6A). Interestingly, this acetylated lysine (K230) of p150^{Glued} lies in coiled-coil region 1 (CC1), the domain responsible for binding the DIC (King et al., 2003; Karki and Holzbaur, 1995). This region is highly conserved across species from flies through humans, emphasizing its importance (Figure 6B). As shown in Figures 6C and 6D, inhibition of HDAC1 in HEK293 cells increased the acetylation of p150^{Glued}, while over-expression of HDAC1 decreased the level of acetylation. These results support the hypothesis that HDAC1 promotes deacetylation of p150^{Glued}.

Since HDAC1 activity was required for the retrograde degeneration signal activated by p75NTR (Figure 3), we hypothesized that BDNF would promote HDAC1-dependent deacetylation of p150^{Glued} in sympathetic neurons. We found a significant decrease in the level of acetylated p150^{Glued} following BDNF treatment, and the reduction could be completely prevented by MS275 (Figure 6E), suggesting that p75NTR activation results in p150^{Glued} deacetylation by HDAC1. We also evaluated acetylated tubulin, since HDAC5 and HDAC6 can deacetylate microtubules to regulate axonal transport (Cho and Cavalli, 2014); however, there was no change in the expression or acetylation levels of tubulin following BDNF treatment, indicating that activation of p75NTR does not affect these other HDACs.

Deacetylation of p150^{Glued} Enhances Its Interaction with Dynein

Retrograde signaling typically depends on active transport of the signaling components by the dynein-dynactin complex. To determine if the retrograde degenerative signal induced by p75NTR activation was dependent on dynein, we tested the inhibitor ciliobrevin A, which blocks the ATPase activity of dynein without affecting kinesins (Firestone et al., 2012). When distal axons were treated with ciliobrevin A, there was a significant reduction in BDNF-induced apoptosis (Figure 7A), indicating that the retrograde signal generated by p75NTR was dynein dependent.

Since the lysine (K230) on p150^{Glued} that we found acetylated in the presence of MS275 lies in the CC1 domain, which interacts with the DIC, we hypothesized that deacetylation of p150^{Glued} by HDAC1 affects its interaction with dynein. In HEK293 cells treated with MS275, there was a significant decrease in the association of p150^{Glued} with DIC relative to untreated cells, suggesting that the acetylation reduces their interaction (Figure 7B). Similarly, we treated the neurons with BDNF to stimulate deacetylation of p150^{Glued}, or NGF+MS275, to maximize the acetylation. In the presence of BDNF, there was a significant increase in the co-immunoprecipitation of p150^{Glued} and DIC compared to NGF+MS275, supporting a role for p75NTR in regulating this interaction (Figure 7C).

To specifically address the influence of K230 acetylation on p150^{Glued} binding to dynein, we mutated K230 either to arginine (R), which cannot be acetylated, or glutamine (Q), which can mimic an acetylated lysine (Fujimoto et al., 2012). Wild-type p150^{Glued} or the mutants were transfected into HEK293 cells and their ability to pull down with DIC was quantified (Figure 7D). The p150^{Glued}-dynein interaction was not significantly altered by the K230Q mutation, which we suggest indicated that glutamine does not adequately mimic acetyl-lysine in this system, as reported earlier for the protein Ku (Fujimoto et al., 2012). However, the K230R mutant associated with dynein significantly better than the wild-type p150^{Glued}, supporting the notion that deacetylation of K230 increases the formation of the p150^{Glued}-dynein complex, which is required for retrograde apoptotic signaling.

DISCUSSION

In this study, we identify an HDAC1-dependent signal downstream of the p75NTR as critical for the regulation of retrograde, pro-apoptotic signals generated in response to p75NTR

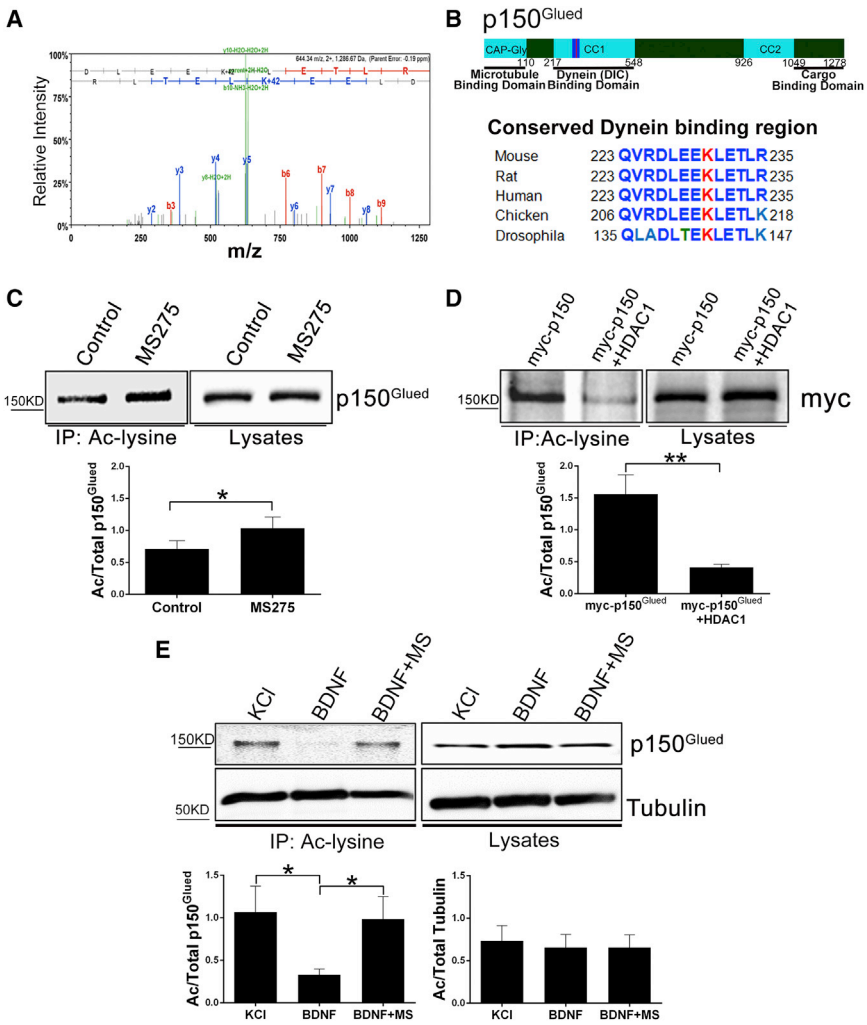

Figure 6. HDAC1 Deacetylates p150^{Glued} at Lysine 230

(A) MS/MS spectrum of acetylated p150^{Glued} tryptic peptide spanning lysine 230. Annotated product ions highlighted in red and blue correspond to b- and y-type ions, respectively. Neutral loss ions from the peptide precursor or product ions are highlighted in green. The observed product ions confirmed acetylation at K230 as indicated by a 42-Da mass shift.

(B) (Top) Schematic of p150^{Glued}. (Bottom) Comparison of protein sequences from the DIC binding region of CC1 around K230 from the indicated species.

(C) Inhibition of HDAC1 increases the acetylation of p150^{Glued}. (Top) HEK293 cells were treated +/- MS275 for 48 hr and then fractionated, and cytosolic lysates were immunoprecipitated with anti-acetyl lysine and western blotted for p150^{Glued}. (Bottom) Bar graph showing the average ratio of acetylated over total p150^{Glued} ± SEM for n = 7; *, $p < 0.05$, Student's t test.

(D) Over-expression of HDAC1 reduces the amount of acetylated p150^{Glued}. (Top) HEK293 cells were transfected with Myc-p150^{Glued} with or without HDAC1-Flag. The cytosolic lysates were immunoprecipitated with anti-acetyl lysine and western blotted with an antibody to Myc. (Bottom) The average ratio of acetylated over total p150^{Glued} ± SEM for n = 5; **, $p < 0.01$, Student's t test.

(E) Activation of p75NTR reduces the level of acetylated p150^{Glued}. Sympathetic neurons were treated with 12.5 mM KCl or 200 ng/mL BDNF +/- 5 μm MS275 (MS) for 48 hr. The neurons were fractionated, and the cytosolic lysates were immunoprecipitated with anti-acetyl lysine and western blotted for p150^{Glued} or alpha-Tubulin. (Top) Representative western blot image. (Bottom) The average ratio of acetylated over total p150^{Glued} or tubulin ± SEM for n = 6–7; *, $p < 0.05$, Student's t test.

activation by ligand binding or TFD in distal axons (Figure 7E). The involvement of p75NTR in retrograde pro-apoptotic signaling following TFD helps to explain previous findings that sensory and sympathetic neurons in *trkA*$^{-/-}$ (Ntrk1$^{-/-}$) mice could be rescued by simultaneous deletion of *p75ntr* (Ngfr) (Majdan et al., 2001; Nikoletopoulou et al., 2010). The loss of TrkA mimics TFD during development; therefore, based on our results, elimination of p75NTR would reduce pro-apoptotic signaling. Notably, neurons engineered to express TrkA underwent apoptosis in the absence of NGF. The cell death correlated with p75NTR cleavage and could be prevented by a γ-secretase inhibitor, suggesting that p75NTR cleavage contributed to the apoptosis (Nikoletopoulou et al., 2010). The mechanism by which loss of TrkA signaling induces p75NTR cleavage and retrograde signaling is not known. However, withdrawal of NGF activates JNK (Xia et al., 1995), which can stimulate the cleavage of p75NTR, in part, through up-regulation and activation of α-secretase (Kenchappa et al., 2010). It is possible that local activation of JNK causes the release of the p75NTR ICD, which then forms a retrograde signaling complex.

Direct activation of p75NTR by ligand binding has also been shown to induce retrograde degenerative signaling. For example, pro-neurotrophin-3 applied exclusively to distal axons of sympathetic neurons induced apoptosis via p75NTR (Yano et al., 2009), and *in vivo* activation of p75NTR was suggested to contribute to the normal developmental pruning of motor neurons (Taylor et al., 2012). The nature of the retrograde apoptotic signal was not investigated in those studies; however, our results indicate that activation of p75NTR exclusively in axons induces retrograde transport of the p75NTR ICD, which promotes neuronal apoptosis. Indeed, expression of p75NTR ICD alone in sympathetic neurons (including both cell bodies and axons) leads to their death (Kenchappa et al., 2006), and mice engineered to ectopically express the p75NTR ICD in neurons exhibited extensive, global neuron loss (Majdan et al., 1997).

Although apoptosis induced by NGF withdrawal or direct activation of p75NTR both involve cleavage of p75NTR and retrograde transport of the ICD, there are distinct differences between the mechanisms by which apoptosis is ultimately induced. For example, both p75NTR activation by ligand binding and TFD stimulate phosphorylation of c-Jun by JNK; however, c-Jun is only necessary for apoptosis induced by TFD (Palmada et al., 2002). Certainly, multiple signals are generated by these two processes that influence the fate of the cell; nevertheless,

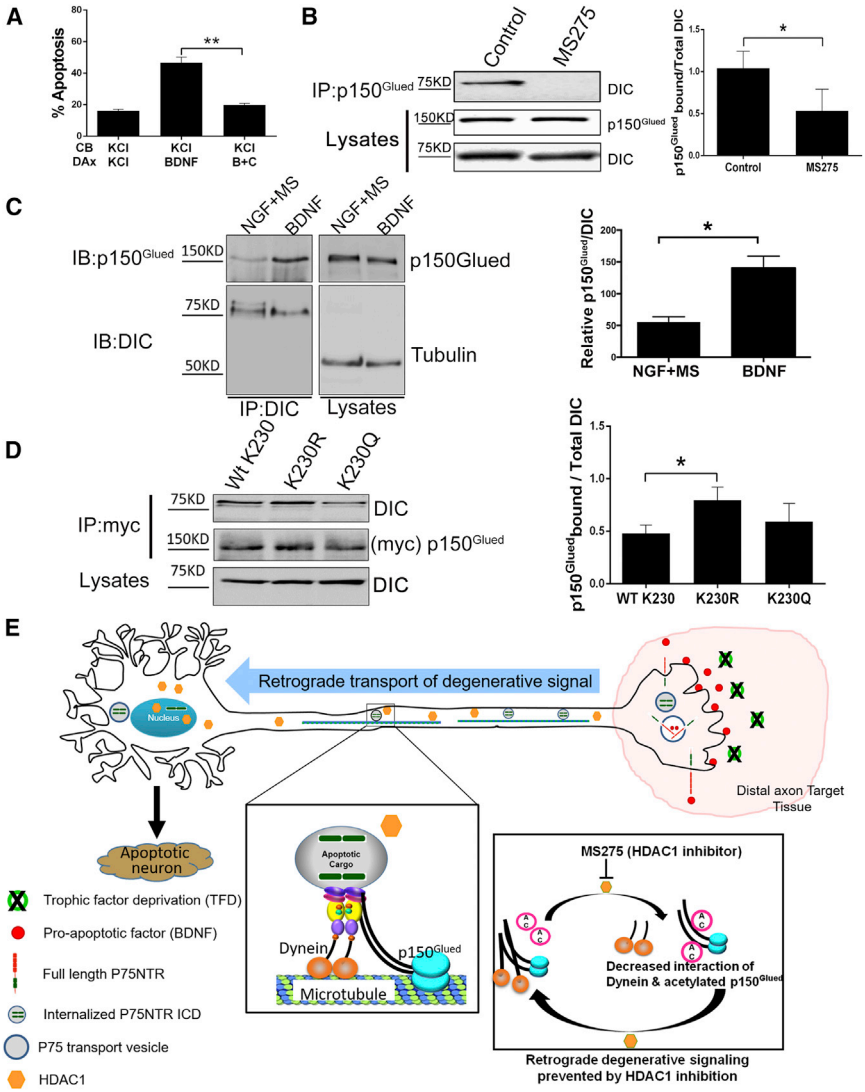

Figure 7. Deacetylation of p150^{Glued} Increases Its Interaction with Dynein

(A) Inhibition of dynein blocks p75NTR retrograde apoptotic signaling. Sympathetic neurons were cultured in microfluidic chambers, and cell bodies (CB) and distal axons (DAx) were treated with 12.5 mM KCl (K) or 200 ng/mL BDNF, as indicated. During the last 8 hr, 25 μm ciliobrevin A, together with BDNF, was applied to the DAx (B+C). The neurons were then fixed and stained for TUJ1 and DAPI to quantify pyknotic nuclei. The bars depict the means ± SEM for n = 3; **, p < 0.01; 2-way ANOVA with Tukey's multiple comparisons test.

(B) Inhibition of HDAC1 reduces the interaction of p150^{Glued} with dynein. (Left) HEK293 cells were treated with MS275 or left untreated (control) and then fractionated, and the cytosolic lysates were immunoprecipitated with anti-p150^{Glued}, then western blotted for DIC. Also shown are the lysates blotted for p150^{Glued} and DIC. (Right) The average ratio of DIC pulled down to total DIC in the lysates ± SEM for n = 3; *, p < 0.05, Student's t test.

(C) Activation of p75NTR enhances the interaction of p150^{Glued} with dynein. (Left) Neurons were treated with 200 ng/mL BDNF or 20 ng/mL NGF + 5 μM MS275 for 48 hr. The neurons were then lysed and immunoprecipitated with DIC and western blotted for p150^{Glued} or DIC. (Right) The average ratio of p150^{Glued} pulled down with DIC to the total DIC in the lysates ± SEM for n = 3; *, p < 0.05, Student's t test.

(D) Mutation of K230 to R in p150^{Glued} increases its interaction with dynein. (Left) HEK293 cells were transfected with Myc-p150^{Glued} wild-type, K230R, or K230Q mutant. The cells were then fractionated, and the cytosolic lysates immunoprecipitated with anti-Myc and western blotted for DIC or p150^{Glued}, as indicated. Also shown are the lysates blotted for DIC. (Right) The average ratio of DIC pulled down to the total DIC in the lysates ± SEM for n = 6; *, p < 0.05, Student's t test.

(E) Summary model. Axonal HDAC1 is required for retrograde apoptotic signaling by activation of p75NTR or trophic factor deprivation. HDAC1 enhances p75 ICD transport in axons by deacetylating p150^{Glued}, which facilitates its binding to the dynein intermediate chain.

both include a pro-apoptotic signal involving JNK and the proteolytic cleavage of p75NTR.

The proteolysis of p75NTR by γ-secretase was reported to occur in endosomes following internalization in PC12 cells (Urra et al., 2007). Therefore, we expect that the p75NTR ICD is generated on endosomes within the axon, although this remains to be determined. In contrast, cleavage of many substrates by α-secretase occurs at the plasma membrane (Murphy, 2008); thus, the shedding of p75NTR's ECD by α-secretase may occur at the axon surface, which would explain why we detected so little free ECD in the axons. Interestingly, p75NTR has been detected in MVBs following endocytosis (Butowt and Bartheld, 2009; Escudero et al., 2014). In neurons of the avian isthmo-optic nucleus, which innervate the retina, p75NTR activation by NGF on axon ends in the eye resulted in apoptosis (von Bartheld et al., 1994). This retrograde p75NTR-mediated cell death correlated with accumulation of NGF in the neuronal soma in MVBs (Butowt and Bartheld, 2009), suggesting that retrograde transport of p75NTR (and possibly separated ECD and ICD) occurs in MVBs. The increase in co-localization of p75NTR ICD and CD63 we observed in axons following BDNF treatment or TFD suggests that the retrograde degenerative signal is transported in MVBs, although we cannot rule out the involvement of other vesicles.

How the freed ICD would remain associated with a vesicle is not clear, since this fragment would be released following receptor cleavage. However, it is notable that there is a palmitoylation site in the juxtamembrane region of the ICD that is required for cell death signaling (Underwood et al., 2008). The addition of this lipid may allow the ICD to associate with a vesicle for transport. An analogous mechanism was recently reported for DLK: following axonal injury of sensory neurons, DLK was palmitoylated, which facilitated its recruitment to vesicles for retrograde transport (Holland et al., 2016).

Our findings also reveal that axonal HDAC1 is required for pro-apoptotic retrograde signaling. Although HDAC1 has been considered exclusively nuclear, it was recently reported that this deacetylase can translocate out of the nucleus into the axons of hippocampal and cortical neurons following exposure to toxic insults, such as TNF and glutamate (Kim et al., 2010). In these axons, HDAC1 promoted degeneration by disrupting mitochondrial transport through binding to the kinesins KIF2a and KIF5. In contrast, we found HDAC1 is constitutively present in sympathetic axons, even under strong pro-survival signaling. The constitutive presence of HDAC1 in sympathetic axons may reflect a general difference between peripheral and central axons; however, there must be some mechanism in the peripheral axons to prevent the deacetylase from disrupting mitochondrial transport. In the central nervous system, HDAC1 may promote degeneration by two mechanisms: disrupting mitochondrial transport and enhancing retrograde degenerative signaling. Since most cargos bind both kinesins and dynein (Maday et al., 2014), sequestering the anterograde motors KIF2a and KIF5 may result in a predominance of dynein associated with some cargo, leading to primarily retrograde transport, although this remains to be investigated.

In an effort to understand the role of HDAC1 in regulating p75ICD transport, we identified the dynactin subunit p150^{Glued} as a potential substrate. p150^{Glued} is the largest subunit of the 1 MDa dynactin complex, which is essential for virtually all aspects of dynein function (Carter et al., 2016; King and Schroer, 2000; Schroer, 2004; Urnavicius et al., 2015). In its N-terminus, p150^{Glued} contains a cytoskeleton-associated protein Gly-rich domain, which binds microtubules, followed by two coiled-coil domains, the first of which (CC1) binds directly to the DIC. Our results indicate that p150^{Glued} can be acetylated at K230, in the CC1 region, and deacetylation of K230 increased its association with DIC.

The deacetylation of p150^{Glued} was enhanced following BDNF treatment, and this could be prevented by inhibition of HDAC1. The mechanism by which p75NTR induces HDAC1-dependent deacetylation of p150^{Glued} is not known; however, an association between HDAC1 and the p75NTR-interacting protein SC1 has previously been reported (Chittka et al., 2004). SC1 is a transcription factor that associates with the ICD of p75NTR and translocates to the nucleus upon neurotrophin binding to p75NTR (Chittka et al., 2004). Therefore, activation of the receptor may lead to recruitment of HDAC1 through association with SC1.

It is interesting to consider the clinical implications of these results. Notably, the ICD of p75NTR was previously identified in association with dynein in the axons of mice harboring the G93A mutation in superoxide dismutase 1 (SOD1) that is associated with a form of amyotrophic lateral sclerosis, but not wild-type mice (Perlson et al., 2009, 2010). Inhibition of this retrograde signaling rescued cultured motor neurons expressing the mutant SOD1. Hence, axonal transport of both pro-survival and pro-apoptotic signals needs to be considered in designing therapeutic strategies for neurodegenerative conditions.

STAR★METHODS

Detailed methods are provided in the online version of this paper and include the following:

SUPPLEMENTAL INFORMATION

Supplemental information includes three figures and can be found with this article online at https://doi.org/10.1016/j.devcel.2018.07.001.

ACKNOWLEDGMENTS

The authors thank members of the Carter lab for helpful discussions and Vanderbilt Mass Spectrometry Research Center Proteomics Core Facility for data acquisition on an LTQ Orbitrap Velos mass spectrometer funded by the NIH (S10RR027714). We acknowledge help from Michael Mercier for construct characterization. We are also grateful to the Cell Imaging Shared Resource at Vanderbilt University (supported by NIH grants CA68485, DK20593, DK58404, DK59637, and EY08126). This work was supported by a grant from the Knights Templar Eye Foundation to A.P. and grants from the NIH (R01 NS038220 and R01 NS102365 to B.D.C.; R35 NS097976 to K.A.; R01 EY024373 to S.F.; and R37 NS42925 to P.C.).

AUTHOR CONTRIBUTIONS

A.P. and B.D.C. conceived the project, designed the experiments, and wrote the manuscript. A.P. performed and analyzed the majority of the experiments with help from E.M.S., F.E.H., and N.W. B.B., D.L., K.A., S.G., E.P., S.F., F.B., and P.C. contributed critical reagents and suggestions. D.T.B. helped in designing the experiments, analyzing the data, and writing the manuscript. All authors reviewed and edited the manuscript.

DECLARATION OF INTERESTS

The authors declare no competing interests.

Received: January 28, 2017
Revised: May 19, 2018
Accepted: July 1, 2018
Published: August 06, 2018

REFERENCES

Bertrand, P. (2010). Inside HDAC with HDAC inhibitors. Eur. J. Med. Chem. *45*, 2095–2116.

Butowt, R., and Bartheld, C.S. von (2009). Fates of neurotrophins after retrograde axonal transport: phosphorylation of p75NTR is a sorting signal for delayed degradation. J. Neurosci. *29*, 10715–10729.

Carter, A.P., Diamant, A.G., and Urnavicius, L. (2016). How dynein and dynactin transport cargos: a structural perspective. Curr. Opin. Struct. Biol. *37*, 62–70.

Ceni, C., Unsain, N., Zeinieh, M.P., and Barker, P.A. (2014). Neurotrophins in the regulation of cellular survival and death. Handb. Exp. Pharmacol. *220*, 193–221.

Chevalier-Larsen, E.S., Wallace, K.E., Pennise, C.R., and Holzbaur, E.L.F. (2008). Lysosomal proliferation and distal degeneration in motor neurons expressing the G59S mutation in the p150Glued subunit of dynactin. Hum. Mol. Genet. *17*, 1946–1955.

Chittka, A., Arevalo, J.C., Rodriguez-Guzman, M., Pérez, P., Chao, M.V., and Sendtner, M. (2004). The p75NTR-interacting protein SC1 inhibits cell cycle progression by transcriptional repression of cyclin E. J. Cell Biol. *164*, 985–996.

Cho, Y., and Cavalli, V. (2014). HDAC signaling in neuronal development and axon regeneration. Curr. Opin. Neurobiol. *27*, 118–126.

Deckwerth, T.L., and Johnson, E.M. (1993). Temporal analysis of events associated with programmed cell death (apoptosis) of sympathetic neurons deprived of nerve growth factor. J. Cell Biol. *123*, 1207–1222.

Deinhardt, K., and Chao, M.V. (2014). Trk receptors. In Neurotrophic Factors, G.R. Lewin and B.D. Carter, eds. (Berlin Heidelberg: Springer), pp. 103–119.

Deinhardt, K., Reversi, A., Berninghausen, O., Hopkins, C.R., and Schiavo, G. (2007). Neurotrophins redirect p75NTR from a clathrin-independent to a clathrin-dependent endocytic pathway coupled to axonal transport. Traffic *8*, 1736–1749.

Deppmann, C.D., Mihalas, S., Sharma, N., Lonze, B.E., Niebur, E., and Ginty, D.D. (2008). A model for neuronal competition During development. Science *320*, 369–373.

Emiliani, S., Fischle, W., Van Lint, C., Al-Abed, Y., and Verdin, E. (1998). Characterization of a human RPD3 ortholog, HDAC3. Proc. Natl. Acad. Sci. USA *95*, 2795–2800.

Escudero, C.A., Lazo, O.M., Galleguillos, C., Parraguez, J.I., Lopez-Verrilli, M.A., Cabeza, C., Leon, L., Saeed, U., Retamal, C., Gonzalez, A., et al. (2014). The p75 neurotrophin receptor evades the endolysosomal route in neuronal cells, favouring multivesicular bodies specialised for exosomal release. J. Cell Sci. *127*, 1966–1979.

Firestone, A.J., Weinger, J.S., Maldonado, M., Barlan, K., Langston, L.D., O'Donnell, M., Gelfand, V.I., Kapoor, T.M., and Chen, J.K. (2012). Small-molecule inhibitors of the AAA+ ATPase motor cytoplasmic dynein. Nature *484*, 125–129.

Fujimoto, H., Higuchi, M., Koike, M., Ode, H., Pinak, M., Bunta, J.K., Nemoto, T., Sakudoh, T., Honda, N., Maekawa, H., et al. (2012). A possible overestimation of the effect of acetylation on lysine residues in KQ mutant analysis. J. Comput. Chem. *33*, 239–246.

Ghosh, A.S., Wang, B., Pozniak, C.D., Chen, M., Watts, R.J., and Lewcock, J.W. (2011). DLK induces developmental neuronal degeneration via selective regulation of proapoptotic JNK activity. J. Cell Biol. *194*, 751–764.

Haberland, M., Montgomery, R.L., and Olson, E.N. (2009). The many roles of histone deacetylases in development and physiology: implications for disease and therapy. Nat. Rev. Genet. *10*, 32–42.

Harrington, A.W., and Ginty, D.D. (2013). Long-distance retrograde neurotrophic factor signalling in neurons. Nat. Rev. Neurosci. *14*, 177–187.

Hempstead, B.L., Martin-Zanca, D., Kaplan, D.R., Parada, L.F., and Chao, M.V. (1991). High-affinity NGF binding requires coexpression of the trk proto-oncogene and the low-affinity NGF receptor. Nature *350*, 678–683.

Hibbert, A.P., Kramer, B.M.R., Miller, F.D., and Kaplan, D.R. (2006). The localization, trafficking and retrograde transport of BDNF bound to p75NTR in sympathetic neurons. Mol. Cell. Neurosci. *32*, 387–402.

Holland, S.M., Collura, K.M., Ketschek, A., Noma, K., Ferguson, T.A., Jin, Y., Gallo, G., and Thomas, G.M. (2016). Palmitoylation controls DLK localization, interactions and activity to ensure effective axonal injury signaling. Proc. Natl. Acad. Sci. USA *113*, 763–768.

Hu, E., Dul, E., Sung, C.M., Chen, Z., Kirkpatrick, R., Zhang, G.F., Johanson, K., Liu, R., Lago, A., Hofmann, G., et al. (2003). Identification of novel isoform-selective inhibitors within Class I histone deacetylases. J. Pharmacol. Exp. Ther. *307*, 720–728.

Jung, K.M., Tan, S., Landman, N., Petrova, K., Murray, S., Lewis, R., Kim, P.K., Kim, D.S., Ryu, S.H., Chao, M.V., et al. (2003). Regulated intramembrane proteolysis of the p75 neurotrophin receptor modulates its association with the TrkA receptor. J. Biol. Chem. *278*, 42161–42169.

Kanning, K.C., Hudson, M., Amieux, P.S., Wiley, J.C., Bothwell, M., and Schecterson, L.C. (2003). Proteolytic processing of the p75 neurotrophin receptor and two homologs generates C-terminal fragments with signaling capability. J. Neurosci. *23*, 5425–5436.

Karki, S., and Holzbaur, E.L.F. (1995). Affinity Chromatography demonstrates a direct binding between cytoplasmic dynein and the dynactin complex. J. Biol. Chem. *270*, 28806–28811.

Kenchappa, R.S., Tep, C., Korade, Z., Urra, S., Bronfman, F.C., Yoon, S.O., and Carter, B.D. (2010). p75 neurotrophin receptor-mediated apoptosis in sympathetic neurons involves a biphasic activation of JNK and up-regulation of tumor necrosis factor-alpha-converting enzyme/ADAM17. J. Biol. Chem. *285*, 20358–20368.

Kenchappa, R.S., Zampieri, N., Chao, M.V., Barker, P.A., Teng, H.K., Hempstead, B.L., and Carter, B.D. (2006). Ligand-dependent cleavage of the P75 neurotrophin receptor is necessary for NRIF nuclear translocation and apoptosis in sympathetic neurons. Neuron *50*, 219–232.

Kim, J.Y., Shen, S., Dietz, K., He, Y., Howell, O., Reynolds, R., and Casaccia, P. (2010). HDAC1 nuclear export induced by pathological conditions is essential for the onset of axonal damage. Nat. Neurosci. *13*, 180–189.

King, S.J., and Schroer, T.A. (2000). Dynactin increases the processivity of the cytoplasmic dynein motor. Nat. Cell Biol. *2*, 20–24.

King, S.J., Brown, C.L., Maier, K.C., Quintyne, N.J., and Schroer, T.A. (2003). Analysis of the dynein-dynactin interaction in vitro and in vivo. Mol. Biol. Cell *14*, 5089–5097.

Kirchhausen, T., Macia, E., and Pelish, H.E. (2008). Use of Dynasore, the small molecule inhibitor of dynamin, in the regulation of endocytosis. Methods Enzymol. *438*, 77–93.

Kraemer, B.R., Yoon, S.O., and Carter, B.D. (2014). The biological functions and signaling mechanisms of the p75 neurotrophin receptor. Handb. Exp. Pharmacol. *220*, 121–164.

Macia, E., Ehrlich, M., Massol, R., Boucrot, E., Brunner, C., and Kirchhausen, T. (2006). Dynasore, a cell-permeable inhibitor of dynamin. Dev. Cell *10*, 839–850.

Maday, S., Twelvetrees, A.E., Moughamian, A.J., and Holzbaur, E.L.F. (2014). Axonal transport: cargo-specific mechanisms of motility and regulation. Neuron *84*, 292–309.

Majdan, M., Lachance, C., Gloster, A., Aloyz, R., Zeindler, C., Bamji, S., Bhakar, A., Belliveau, D., Fawcett, J., Miller, F.D., et al. (1997). Transgenic mice expressing the intracellular domain of the p75 neurotrophin receptor undergo neuronal apoptosis. J. Neurosci. *17*, 6988–6998.

Majdan, M., Walsh, G.S., Aloyz, R., and Miller, F.D. (2001). TrkA mediates developmental sympathetic neuron survival in vivo by silencing an ongoing p75NTR-mediated death signal. J. Cell Biol. *155*, 1275–1285.

McKenney, R.J., Huynh, W., Tanenbaum, M.E., Bhabha, G., and Vale, R.D. (2014). Activation of cytoplasmic dynein motility by dynactin-cargo adapter complexes. Science *345*, 337–341.

Mobley, B.C., Kwon, M., Kraemer, B.R., Hickman, F.E., Qiao, J., Chung, D.H., and Carter, B.D. (2015). Expression of MYCN in multipotent sympathoadrenal progenitors induces proliferation and neural differentiation, but is not sufficient for tumorigenesis. PLOS ONE *10*, e0133897.

Mok, S.A., Lund, K., and Campenot, R.B. (2009). A retrograde apoptotic signal originating in NGF-deprived distal axons of rat sympathetic neurons in compartmented cultures. Cell Res. *19*, 546–560.

Murphy, G. (2008). The ADAMs: signalling scissors in the tumour microenvironment. Nat. Rev. Cancer *8*, 929–941.

Nikoletopoulou, V., Lickert, H., Frade, J.M., Rencurel, C., Giallonardo, P., Zhang, L., Bibel, M., and Barde, Y.A. (2010). Neurotrophin receptors TrkA and TrkC cause neuronal death whereas TrkB does not. Nature *467*, 59–63.

Palmada, M., Kanwal, S., Rutkoski, N.J., Gustafson-Brown, C., Johnson, R.S., Wisdom, R., and Carter, B.D. (2002). c-jun is essential for sympathetic neuronal death induced by NGF withdrawal but not by p75 activation. J. Cell Biol. *158*, 453–461.

Perlson, E., Jeong, G.B., Ross, J.L., Dixit, R., Wallace, K.E., Kalb, R.G., and Holzbaur, E.L.F. (2009). A switch in retrograde signaling from survival to stress in rapid-onset neurodegeneration. J. Neurosci. *29*, 9903–9917.

Perlson, E., Maday, S., Fu, M.M., Moughamian, A.J., and Holzbaur, E.L.F. (2010). Retrograde axonal transport: pathways to cell death? Trends Neurosci. *33*, 335–344.

Schachtrup, C., Ryu, J.K., Mammadzada, K., Khan, A.S., Carlton, P.M., Perez, A., Christian, F., Le Moan, N., Vagena, E., Baeza-Raja, B., et al. (2015). Nuclear pore complex remodeling by p75(NTR) cleavage controls TGF-β signaling and astrocyte functions. Nat. Neurosci. *18*, 1077–1080.

Schindelin, J., Arganda-Carreras, I., Frise, E., Kaynig, V., Longair, M., Pietzsch, T., Preibisch, S., Rueden, C., Saalfeld, S., Schmid, B., et al. (2012). Fiji: an open-source platform for biological-image analysis. Nat. Methods *9*, 676–682.

Schroer, T.A. (2004). Dynactin. Annu. Rev. Cell Dev. Biol. *20*, 759–779.

Scott-Solomon, E., and Kuruvilla, R. (2018). Mechanisms of neurotrophin trafficking via Trk receptors. Mol. Cell. Neurosci. Published online March 27, 2018.

Simon, D.J., Pitts, J., Hertz, N.T., Yang, J., Yamagishi, Y., Olsen, O., Tešić Mark, M., Molina, H., and Tessier-Lavigne, M. (2016). Axon degeneration gated by retrograde activation of somatic pro-apoptotic signaling. Cell *164*, 1031–1045.

Skeldal, S., Sykes, A.M., Glerup, S., Matusica, D., Palstra, N., Autio, H., Boskovic, Z., Madsen, P., Castrén, E., Nykjaer, A., et al. (2012). Mapping of the interaction site between sortilin and the p75 neurotrophin receptor reveals a regulatory role for the sortilin intracellular domain in p75 neurotrophin receptor shedding and apoptosis. J. Biol. Chem. *287*, 43798–43809.

Tauris, J., Gustafsen, C., Christensen, E.I., Jansen, P., Nykjaer, A., Nyengaard, J.R., Teng, K.K., Schwarz, E., Ovesen, T., Madsen, P., et al. (2011). Proneurotrophin-3 may induce Sortilin-dependent death in inner ear neurons. Eur. J. Neurosci. *33*, 622–631.

Taylor, A.R., Gifondorwa, D.J., Robinson, M.B., Strupe, J.L., Prevette, D., Johnson, J.E., Hempstead, B., Oppenheim, R.W., and Milligan, C.E. (2012). Motoneuron programmed cell death in response to proBDNF. Dev. Neurobiol. *72*, 699–712.

Underwood, C.K., Reid, K., May, L.M., Bartlett, P.F., and Coulson, E.J. (2008). Palmitoylation of the C-terminal fragment of p75NTR regulates death signaling and is required for subsequent cleavage by γ-secretase. Mol. Cell. Neurosci. *37*, 346–358.

Urnavicius, L., Zhang, K., Diamant, A.G., Motz, C., Schlager, M.A., Yu, M., Patel, N.A., Robinson, C.V., and Carter, A.P. (2015). The structure of the dynactin complex and its interaction with dynein. Science *347*, 1441–1446.

Urra, S., Escudero, C.A., Ramos, P., Lisbona, F., Allende, E., Covarrubias, P., Parraguez, J.I., Zampieri, N., Chao, M.V., Annaert, W., et al. (2007). TrkA Receptor Activation by Nerve Growth Factor Induces Shedding of the p75 neurotrophin Receptor Followed by endosomal γ-Secretase-mediated Release of the p75 intracellular Domain. J. Biol. Chem. *282*, 7606–7615.

Vicario, A., Kisiswa, L., Tann, J.Y., Kelly, C.E., and Ibáñez, C.F. (2015). Neuron-type-specific signaling by the p75NTR death receptors is regulated by differential proteolytic cleavage. J. Cell Sci. *128*, 1507–1517.

von Bartheld, C.S., Kinoshita, Y., Prevette, D., Yin, Q.W., Oppenheim, R.W., and Bothwell, M. (1994). Positive and negative effects of neurotrophins on the isthmo-optic nucleus in chick embryos. Neuron *12*, 639–654.

Wu, C., Cui, B., He, L., Chen, L., and Mobley, W.C. (2009). The coming of age of axonal neurotrophin signaling endosomes. J. Proteomics *72*, 46–55.

Xia, Z., Dickens, M., Raingeaud, J., Davis, R.J., and Greenberg, M.E. (1995). Opposing effects of ERK and JNK-p38 MAP kinases on apoptosis. Science *270*, 1326–1331.

Yano, H., Torkin, R., Martin, L.A., Chao, M.V., and Teng, K.K. (2009). Proneurotrophin-3 is a neuronal apoptotic ligand: evidence for retrograde-directed cell killing. J. Neurosci. *29*, 14790–14802.

d'Ydewalle, C., Krishnan, J., Chiheb, D.M., Van Damme, P., Irobi, J., Kozikowski, A.P., Vanden Berghe, P.V., Timmerman, V., Robberecht, W., and Van Den Bosch, L. (2011). HDAC6 inhibitors reverse axonal loss in a mouse model of mutant HSPB1-induced Charcot-Marie-Tooth disease. Nat. Med. *17*, 968–974.

Ye, M., Lehigh, K.M., and Ginty, D.D. (2018). Multivesicular bodies mediate long-range retrograde NGF-TrkA signaling. eLife *7*, e33012.

Zheng, J.Q., Kelly, T.K., Chang, B., Ryazantsev, S., Rajasekaran, A.K., Martin, K.C., and Twiss, J.L. (2001). A functional role for intra-axonal protein synthesis during axonal regeneration from adult sensory neurons. J. Neurosci. *21*, 9291–9303.

Zhu, Y., Vidaurre, O.G., Adula, K.P., Kezunovic, N., Wentling, M., Huntley, G.W., and Casaccia, P. (2017). Subcellular distribution of HDAC1 in neurotoxic conditions is dependent on serine phosphorylation. J. Neurosci. *37*, 7547–7559.

STAR★METHODS

KEY RESOURCES TABLE

REAGENT or RESOURCE	SOURCE	IDENTIFIER
Antibodies		
Rabbit anti-HDAC1	Santa cruz	Cat#sc-7872; RRID:AB_2279709
Mouse anti-TUJ1	Covance	Cat#MMS-435P; RRID AB_2313773
Rabbit anti-Histone H3	Abcam	Cat# ab46765; RRID:AB_880439
Mouse anti-Tau	Cell signaling Technology	Cat# 4019; RRID:AB_2281791
Rabbit anti-P75NTR ICD	Laboratory of Bruce D Carter Kenchappa et al., 2006	N/A
Mouse anti-p150^{Glued}	BD Biosciences	Cat# 610474; RRID:AB_397846
Mouse anti-Tubulin	Millipore	Cat# CP06; RRID:AB_2617116
Mouse anti-myc	Cell signaling Technology	Cat# 2276; RRID:AB_331783
Mouse anti-HDAC1	Millipore	Cat# 05-100; RRID:AB_916345
Mouse anti-Dynein	Millipore	Cat# MAB1618; RRID:AB_2246059
Rabbit anti-CD63	Santa Cruz Biotechnology	Cat# sc-15363; RRID:AB_648179
Rabbit anti-P75NTR	Alomone Labs	Cat# ANT-007-AO; RRID:AB_2039966
Mouse anti p75 NTR ECD antibody tagged with FITC	Santa Cruz Biotechnology	Cat# sc-53631; RRID:AB_784824
Mouse anti-NGF	Millipore	Cat# MAB5260Z; RRID:AB_95190
Goat anti-Rabbit IgG (H+L) Cross-Adsorbed Secondary Antibody, HRP	Thermo Fisher Scientific	Cat# 31462; RRID:AB_228338
Goat anti-Mouse IgG (H+L), HRP Conjugate Secondary antibody	Promega	Cat# W4021; RRID:AB_430834
Goat anti-Rabbit IgG (H+L) Antibody, Alexa Fluor 546 Conjugated	Molecular Probes	Cat# A-11010; RRID:AB_143156
Goat anti-Rabbit IgG (H+L) Highly Cross-adsorbed Antibody, Alexa Fluor 647 Conjugated	Molecular Probes	Cat# A-21245; RRID:AB_141775
Goat anti-Mouse IgG2a Cross-Adsorbed Secondary Antibody, Alexa Fluor 488	Thermo Fisher Scientific	Cat# A-21131; RRID:AB_2535771
Bacterial and Virus Strains		
HDAC1 shRNA	Laboratory of Patrizia Casaccia Kim et al., 2010	N/A
GFP control Virus	Laboratory of Bruce D. Carter Mobley et al., 2015	N/A
P75 Lentivirus	Laboratory of Eran Perlson This paper	N/A
Chemicals, Peptides, and Recombinant Proteins		
NGF 2.5S	Invitrogen	Cat#13257-019
BDNF	Gifted from Regeneron	N/A
Cholera ToxinB	Invitrogen	Cat# C-34778
Cytosine arabinofuranoside	Sigma	Cat# C1768
MS275	Cayman Chemical	Cat# 13284
Sodium butyrate	Sigma Aldrich	Cat# B5887
Tubastatin A	Cayman Chemical	Cat# 10559
Dynasore	Sigma	Cat# D7693
DAPT (N-[N-(3,5-Difluorophenacetyl)-L-alanyl]-S-phenylglycine t-butyl ester)	Millipore	Cat# 565770
Ciliobrevin A (HPI-4)	Sigma	Cat# H4541
Acetyl lysine Agarose Beads	Immunechem	Cat# ICP0388
Trypsin	Worthington Biochemical	Cat# 3708

(*Continued on next page*)

Continued

REAGENT or RESOURCE	SOURCE	IDENTIFIER
Collagenase	Sigma	Cat# C9891
Poly D Lysine	M P Biomedicals	Cat# 150175
Laminin	Invitrogen	Cat# 23017-015
Ultra-culture media	Lonza	Cat# 12-725F
High glucose DMEM media	Molecular and Cell Biology Resource Core, Vanderbilt university Medical Centre	N/A
Potassium Chloride	E M Sciences	Cat# PX1405-5
Para formaldehyde	Sigma	Cat# P6148
Lipofectamine 2000 Transfection reagent	Invitrogen	Cat# 11668027
Bovine Serum Albumin	Sigma	Cat# A3059
Normal Goat serum	M P Biomedicals	Cat# 2191356
Fish Gelatin	Sigma	Cat# G7765
Urea	Acros Organics	Cat# 327380010
Tris Buffer	Fisher Scientific	Cat# BP152-500
Trifluoro ethanol (TFE)	Acros Organics	Cat# 139750250
Iodo acetamide	Sigma-Aldrich	Cat# I1149-25G
Proteomics grade Trypsin	Promega	Cat# V5280
Tri fluoro acetate	Thermo Scientific	Cat# 28904
Sep-pak SPE material	Waters	Cat# WAT036790
Acetonitrile	Honeywell (Burdick & Jackson)	Cat# 015-1L
360x150 um Fused Silica	Polymicro Technologies	Cat# 1068150024
Filter end fitting	IDEX	Cat# M-120X
Luna SCX Material	Phenomenex	Cat# 04A-4398
Jupiter C18 Material	Phenomenex	04A-4263
Microfilter Union	IDEX	M-520
360x100 um Fused Silica	Polymicro Technologies	1068150023
Nonidet P-40	Sigma	Cat# I8896
Mini EDTA free protease inhibitor mixture tablet	Roche	Cat# 04693159001
PhosStop phosphatase inhibitor mixture tablet	Roche	Cat# 04906845001
DAPI	Sigma	Cat# 32670
Critical Commercial Assays		
Rat neuron nucleo factor Kit	Lonza	Cat# VPG-1003
Experimental Models: Cell Lines		
HEK 293 cells	ATCC	Cat# CRL-1573, RRID:CVCL_0045
Experimental Models: Organisms/Strains		
SD Rattus norvegicus	Charles River Laboratories, RGD	RGD Cat# 737891; RRID:RGD_737891
CD1(ICR) Mus musculus	IMSR	Cat# CRL:22; RRID:IMSR_CRL:22
CD(SD) Rattus norvegicus	Charles River Laboratories, RGD	RGD Cat# 734476; RRID:RGD_734476
Oligonucleotides		
mCherry-p75NTR-GFP Sequencing Primer 5'- CACCATCGTGGAACAGTACG-3'	This paper	N/A
Primer: V243D mutant generation from rat mCherry-p75NTR-GFP construct 5'- AGCTCCCAGCCTGATGTGACCCGCGGCA-3'	This paper	N/A
Primer: D243N mutant generation from rat mCherry-p75NTR-GFP construct 5'- GCAGCTCCCAGCCTAATGTGACCCGCGGC-3'	This paper	N/A
$p150^{Glued}$ Sequencing Primer 1 5'-GAGGAGGAGGGACTAAGGGCTC-3'	This paper	N/A

(*Continued on next page*)

Continued

REAGENT or RESOURCE	SOURCE	IDENTIFIER
p150^{Glued} Sequencing Primer 2 5'-GAGGAGATGGTGGAGATGCTGACAG-3'	This paper	N/A
p150^{Glued} Sequencing Primer 3 5'-GCCCTCTCTCAGTGCAGTGTGGATG-3'	This paper	N/A
p150^{Glued} Sequencing Primer 4 5'-GCTGAAGGCCTGGGTTTGAAGCTCG-3'	This paper	N/A
p150^{Glued} Sequencing Primer 5 5'-GAGCACACACACGCACGTAGTAGAC-3'	This paper	N/A
Recombinant DNA		
Wildtype mCherry-p75NTR-GFP	Laboratory of Katerina Akassoglou Schachtrup et al., 2015	N/A
Non cleavable V243D mutant mcherry p75 GFP construct	This paper	N/A
Non cleavable V243N mutant mcherry p75 GFP construct	This paper	N/A
HDAC1 flag construct	Emiliani et al., 1998	Addgene Plasmid # 13820
Wild type Myc tagged P150^{Glued} construct	Laboratory of Eran Perlson Chevalier-Larsen et al., 2008	N/A
K230Q mutant Myc tagged p150^{Glued} construct	This paper	N/A
K230R mutant Myc tagged p150^{Glued} construct	This paper	N/A
Software and Algorithms		
ImageJ/FIJI	NIH	https://fiji.sc/
Prism 5	GraphPad	https://www.graphpad.com/scientific-software/prism/
Scaffold 3.0 (Proteome Software)	Proteome software	http://www.proteomesoftware.com/products/scaffold/
Other		
Microfluidic devices	Xona microfluidics	Cat# SND450
Microfluidic devices	Laboratory of Deyu Li	N/A
Cell culture inserts	Millipore	Cat# PIEP30R48
Plasma Cleaner PDC-32G	Harrick Plasma	PDC-32G
Glass bottom dishes	Cellvis	Cat# D35-10-1.5-N
Nucleofactor II electroporation Device	Amaxa	AAD-1001S

CONTACT FOR REAGENT AND RESOURCE SHARING

Further information and requests for resources and reagents should be directed to and will be fulfilled by the Lead Contact, Bruce D. Carter (bruce.carter@vanderbilt.edu). Requests will be handled according to Vanderbilt University and/or NIH policy regarding MTA and related matters.

EXPERIMENTAL MODEL AND SUBJECT DETAILS

Rats and Mice

All animal experiments were approved by the Institutional Animal Care and Use Committee at Vanderbilt University. Wild type, untimed pregnant Sprague Dawley (SD) and CD1 rats and mice were purchased mice from Charles River Laboratory. Pregnant rats and mice were housed in 12-hour day and night cycle environment with ad libitum availability of chow diet and water. Both male and female postnatal day 2-3 old rats and mice were used in all the experiments, other than HDAC1 immunostaining in the nerve where postnatal day 4-5 old rat was used.

Cell Culture

Primary sympathetic neurons from superior cervical ganglia were cultured in UltraCULTURE medium (Lonza) supplemented with 3% fetal bovine serum (Invitrogen), 20 ng/ml nerve growth factor (Harlan), 2 mM L-glutamine (Invitrogen), 100 units/ml penicillin (Invitrogen), and 100 ug/ml streptomycin (Invitrogen) or as indicated.

HEK293 cells were cultured in high glucose DMEM with 10% fetal bovine serum, 100U/ml penicillin and 100 μg/ml streptomycin.

METHOD DETAILS

Cell Culture and Treatments

Sympathetic neurons were isolated from superior cervical ganglia, which were dissected from male and female postnatal day 2-3 rats or mice (murine neurons were used for the HDAC1 knockdown experiment) and dissociated with 0.08% trypsin (Worthington) and 0.3% collagenase (Sigma). Dissociated cells were then plated on poly-d-lysine (MP Biomedicals) and laminin (Invitrogen) coated surface.

For mass cultures, neurons were cultured in UltraCULTURE medium (Lonza) supplemented with 3% fetal bovine serum (Invitrogen), 20 ng/ml nerve growth factor (Harlan), 2 mM L-glutamine (Invitrogen), 100 units/ml penicillin (Invitrogen), and 100 ug/ml streptomycin (Invitrogen) or as indicated. 24 hours after plating, the neurons were treated with 10 uM cytosine arabinofuranoside (AraC) (Sigma) for 24 hrs to inhibit the proliferation of non-neuronal cells. Following 2 days of exposure, AraC was removed and after 12-24 hrs, the neurons were treated at the indicated concentrations with the reagents as described in respective figure legends. For all experiments involving NGF removal and treatment with BDNF or KCl, the neurons were rinsed at least 3 times with media lacking NGF, containing 12.5 mM KCl and 100 ng/ml of anti-NGF with at least 10 min incubation each in between the rinses prior to addition of the indicated reagents. For NGF withdrawal condition, KCl was not included in the media used for washing or treatments.

For neuron cultures in microfluidic devices (from Xona Microfluidics or generated in-house by Deyu Li laboratory, Vanderbilt University School of Engineering), the chambers were sterilized in plasma cleaner (PDC-32G from Harrick Plasma) and assembled on coverslips, then coated with poly D lysine and laminin. Dissociated neurons were plated on one side (proximal) of the devices in ultraCULTURE media with 20 ng/ml NGF and axons were allowed to grow and cross into the other side (distal). To direct the growth of axons more towards the distal side, media with 50 ng/ml NGF was added in the distal compartment for initial two days. We confirmed that there was no diffusion of soluble material between the chambers using a fluorescent dye (Cy3). After the axons reached the distal side, the neurons were kept alive by maintaining the cell bodies in media containing 20 ng/ml or 12.5 mM KCl and distal axons were treated for 48 hours as indicated in figure legends. For infection with HDAC1 shRNA lenti virus, mouse neurons were cultured in microfluidic devices in NGF for 2 days and then incubated with lentivirus expressing HDAC1 shRNA (3.7 $x10^7$ transduction units/ml), GFP control (7.55 $x10^7$ transduction units/ml). After 48 hours of infection, the axons and cell bodies were treated with 200 ng/ml BDNF, 12.5 mM KCl or 20 ng/ml NGF as indicated in figure legends. After the treatments, neurons were fixed in 4% PFA for immunostaining and counting apoptotic nuclei.

The mCherry-p75NTR-GFP construct was kindly provided by Katerina Akassoglou (Gladstone Institute of Neurological Disease, UCSF). The mCherry-p75NTR-GFP reporter construct was expressed in primary sympathetic neurons by electroporation immediately after dissociation of sympathetic neurons using rat neuron nucleofactor kit (Amaxa Cat# VPG-1003) on nucleofactor II device from Amaxa according to manufacturer's instructions. More than 1 million neurons isolated from approximately 20 ganglia were pelleted at 200g for 4 minutes and resuspended in 100 ul of rat neuron nucleofection solution prepared according to manufacturer's instruction. The cell suspension was immediately transferred to Amaxa transfection cuvette containing 20ug of plasmid in small volume of (10-15ul) and zapped on program settings G-013 (designated on the instrument for "rat" neuron DRG). Atleast 1 ml of Ultraculture media with 50 ng/ml NGF was immediately added to the electroporated neurons and the contents were transferred to a 15 ml tube and incubated at 37C in a water bath incubator for at least 20 minutes to promote recovery prior to plating the neurons.

HEK293 cells were cultured in high glucose DMEM with 10% fetal bovine serum and penicillin /streptomycin (100 U/ml, 100 μg/ml, respectively) and transfected using Lipofectamine 2000 (Invitrogen), according to the manufacturer's instructions.

For analysis of p75NTR receptor cleavage, mCherry-p75NTR-GFP wildtype (mCh-p75WT-GFP), V243D mutant (mCh-p75VD-GFP) and V243N mutant (mCh-p75-GFP) constructs were transfected in HEK293 cells. Cells were then pretreated with 10uM ZLLLH for 1 hour (all). For TAPI treatment, cells were pretreated with 10uM TAPI for one hour concurrently with ZLLLH and for PMA treatment, cells were treated with 1uM PMA for 1 hour. After respective treatments, cells were harvested and lysates were prepared for Western blotting.

Isolation of Axons in Culture

To get pure axon fractions without contamination of cell bodies, dissociated neurons were plated on the transwell cell culture inserts with 8 um pore size. Cultured neurons were maintained in 20 ng/ml NGF for 3-4 days. Following the indicated treatment, the axons and cell bodies were separately harvested by scraping the membrane with a cell scrapper. Membrane facing the well contains the axons and the opposite side has cell bodies (Zheng et al., 2001).

Site Directed Mutagenesis of DNA Constructs

To generate non cleavable mCherry-p75NTR-GFP construct, nucleotide changes encoding V243D mutation were introduced into wildtype mCherry-p75NTR-GFP construct (Schachtrup et al, 2015) by site-directed mutagenesis using PfuUltra High-Fidelity DNA polymerase (Agilent Technologies). This V243D mutation was further changed to D243N by site directed mutagenesis PCR, to finally generate the cleavage resistant mCherry-p75NTR-GFP construct with V243N mutation.

To generate the constitutively acetylated mimic construct of $p150^{Glued}$ (K230Q) and non-acetylable $p150^{Glued}$ (K230R), lysine (K) residue of wildtype $p150^{Glued}$ construct at position 230 was changed to glutamine (Q) and arginine (R) respectively by site directed mutagenesis of myc-tagged $p150^{Glued}$ (Chevalier-Larsen, et al, 2008). The accuracy of nucleotides in all the wild type constructs and the changes introduced in the mutant constructs were confirmed by sequencing the wildtype and mutant constructs.

Immunostaining

Primary sympathetic neurons in culture were infected with lentivirus expressing HDAC1 shRNA and/or GFP (control) for more than 48 hrs, then fixed with 4% PFA, permeabilized with 0.1% Triton X-100 containing 0.1% sodium citrate, blocked with 5% BSA or 10% goat serum in PBS, and incubated with antibodies for HDAC1 (1:100) and TUJ1 (1:1000) in PBS containing 0.05% Triton X-100, followed by incubation with fluorescently tagged secondary antibody. Nuclei were visualized by DAPI, and images were acquired with a confocal laser imaging system (LSM 710; Carl Zeiss MicroImaging, Inc.).

Superior cervical ganglia and brain were collected from post-natal day 4-5 rat pups after cardiac perfusion with 4% PFA and embedded in paraffin wax for tissue sectioning. Antigen retrieval of sections was done in citrate buffer (10 mM, pH 6.0). Sections were blocked with 5% BSA and incubated with antibodies for HDAC1 (1:100, Santa cruz biotechnology) and TUJ1 (1:1000, Covance) in PBS containing 0.05% Triton X-100, followed by incubation with fluorescently tagged secondary antibody. Nuclei were visualized by DAPI, and images were acquired with a confocal laser imaging system (LSM 880; Carl Zeiss MicroImaging, Inc.).

For CD63 immunostaining, wildtype mCherry-p75NTR-GFP electroporated neurons were fixed with cold 3% PFA and 4% sucrose and blocked with 5% Fish gelatin in PBS containing 0.1% TritonX 100. Then incubated with CD63 (1:100, Santa cruz biotechnology) antibody followed by incubation with fluorescently tagged secondary antibody. Nuclei were visualized by DAPI, and images were acquired with a confocal laser imaging system (LSM 880; Carl Zeiss MicroImaging, Inc.). Colocalization of P75NTR and CD63 in the axons was counted blindly and 30-40 axons were scored per condition in each experiment.

Neuronal Death Analysis

Following the indicated treatments, sympathetic neurons were fixed with 4% paraformaldehyde and immuno-stained with anti-TUJ1 (1:1000, Covance) primary antibody, Alexa Fluor 488 secondary antibody (1:1000, Invitrogen) and DAPI as nuclear marker. The neurons were scored blindly as apoptotic or non-apoptotic on the basis of the appearance of the nucleus, apoptotic nuclei being condensed or fragmented and much brighter compared to healthy neurons. At least 75-100 TUJ1-positive neurons with their axons crossing to the distal chambers were counted per condition in all experiments in microfluidic devices and mass cultures.

Immuno-Endocytosis of p75NTR

Primary neurons were grown in NGF containing media for 3 days, NGF was then removed and replaced with DMEM containing 1 mg/ml BSA and 12.5 mM KCl for serum deprivation. After 1 hour, anti-p75ECD antibody tagged with FITC (1:50, Santa cruz biotechnology) was added for 1 hour at 4°C. Neurons were then left in KCl or treated with 200 ng/ml BDNF +/- 5μM MS275 for 4 hrs at 37°C, rinsed and incubated at 4°C with Cholera toxin B (1:500, Invitrogen) for 20 min to label the cell surface. Thereafter, the neurons were fixed in 4% paraformaldehyde and processed for TUJ1 immunostaining as described above. The labelled cells were examined and imaged by using a Zeiss LSM 710 confocal microscope with a Plan apochromat 63X/1.4 oil differential interference contrast (DIC) objective. FIJI was used to quantify the cell-associated fluorescence. The total cellular fluorescence was calculated after subtracting the non-specific fluorescence from images of untreated cells obtained with the same illumination and exposure conditions. Internalized p75NTR ECD was determined as the ratio of the internalized receptor (intracellular fluorescence) versus the cell surface-associated receptor (cell-surface-associated fluorescence) and expressed as a percentage of internalized fluorescence (intracellular p75NTR), considering 100% to be the total cell-associated fluorescence.

Live Imaging of Neurons and Kymograph Generation

Sympathetic neurons were electroporated with mCherry-p75NTR-GFP construct and plated on glass bottom dishes. The neurons were first plated in UltraCULTURE media with 50 ng/ml NGF which was changed to media with 20 ng/ml NGF next day. After 2 days in culture, NGF was removed and the neurons were incubated with a p75NTR antibody (Anti-p75NTR (extracellular)-ATTO-550, Alomone labs) for 30 min in phenol red free DMEM with HEPES, BSA (1 mg/ml) and KCl (12.5 mM) on ice. The antibody was then rinsed off and the neurons were treated with or without 200 ng/ml BDNF +/- 5 μM MS275 for 2 hrs.

High-resolution wide-field fluorescence images were acquired on a Nikon Eclipse Ti equipped with a Nikon 100× Plan Apo 1.45 numerical aperture (NA) oil objective and a Nikon DS-Qi2 CMOS camera. Multichannel time lapse images were acquired at 3 sec intervals for a total of 3 min and processed using Nikon Imaging software to generate the kymographs. The cell body is at the top of the kymograph, all sloping (moving) pathways were counted to be moving particles while the horizontal pathways were considered to be stationary. All the kymographs were blindly analyzed to quantify the overall direction of movement. Approximately 100 moving particles were analyzed from at least 8 different neurons in each condition for each experiment.

Analysis of p75NTR Transport Velocity in the Axons

Time lapse image analysis was carried out using FIJI. X-Y coordinates of tracks, distance travelled, velocity were registered from about 40 axons in each experiment using Manual Tracking plugin (Schindelin et al., 2012). Tracks with average velocity < 0.2 um/sec were filtered out. Instantaneous velocities were calculated as the distance a puncta travelled between two consecutive frames, divided by frame interval (3 sec). Velocity distribution is presented for 0.2 μm/sec bins.

p75NTR Receptor Cleavage Analysis in Axons

Primary sympathetic neurons from rats were grown in microfluidic devices and infected with lentivirus with GFP tag on the C-terminal of p75 (provided by Eran Perlson, Tel Aviv University). Upon p75NTR overexpression, distal axons were treated with 200 ng/ml BDNF

or BDNF+ 250nM DAPT for 2 hours and cell bodies were left in 12.5 mM KCl. Distal axons in BDNF+DAPT treatment group were pre-treated with 250nM DAPT alone for 1 hour before BDNF+DAPT treatment. Live neurons were stained with ATTO-550 tagged antibody against p75NTR-ECD and then fixed with 4%PFA. Thereafter, fixed neurons, were stained with GFP and imaged on LSM880 with Airyscan mode. To quantify p75NTR receptor cleavage in axons, green puncta were counted for cleaved p75NTR-ICD and yellow puncta for full length p75NTR receptor.

LC-Tandem MS/MS

Neurons were cultured in trans well cell culture inserts, as described above, to collect the axons. After 2-3 days in 20 ng/ml NGF, 5 μM MS275 was added for 24 hrs to maximize the amount of acetylated HDAC1 substrate. Axon were collected without contamination from cell bodies. Lysates were prepared in 6M urea in 100mM Tris buffer (pH 8.0) and protein concentration was determined.

To prepare tryptic peptides for enrichment, axon lysate (4.7 mg) was diluted 2-fold with trifluoroethanol (TFE). The samples were then reduced by addition of 15 μl of 0.5M TCEP for 1 hr at room temperature, and alkylated with 30 μl of 500 mM iodoacetamide for 30 min in the dark at room temperature. Samples were diluted 10-fold with 100 mM Tris HCl, pH 8.0 and digested overnight at 37°C with proteomics-grade trypsin (Sigma) at a ratio of 1:60 enzyme to protein. The resulting peptides were then desalted by solid-phase extraction (Sep-pak C18 cartridges, Waters Corporation). Digested samples were first acidified with Trifluroacetic acid (TFA), diluted 2-fold with 0.1% TFA, and loaded onto the Sep-pak SPE material. After sample loading, the cartridges were washed with 0.1% TFA, and eluted with acetonitrile containing 0.1% TFA. Eight sequential 1 ml elutions were performed, increasing from 10% up to 80% acetonitrile, and eluates were reduced to dryness via vacuum centrifugation.

Acetylated peptide were enriched essentially as described earlier with minor modifications. Protein-A conjugated agarose beads immobilized with anti-acetyl lysine antibodies (ICP0388; ImmunoChem Pharmaceuticals Inc., Burnaby, British Columbia, Canada) were added at a ratio of 30 μl beads per 2 mg soluble protein resuspended in 1 ml final of NETN buffer (50 mM Tris-HCl [pH 8.0], 100 mM NaCl, 1 mM EDTA, 0.5% NP40) and the mixture was incubated with rotation at 4°C overnight. The beads were washed four times with 1 ml of NETN buffer and three times with ETN (50 mM Tris-HCl [pH 8.0], 100 mM NaCl, 1 mM EDTA). The bound peptides were eluted from the beads by washing three times with 100 μl of 0.1% TFA. The eluates were combined and dried in a SpeedVac.

LC-MS-MS analysis of the peptides was performed using a LTQ-Orbitrap Velos mass spectrometer (Thermo Scientific) equipped with a nanospray source and an Eksigent NanoLC and AS1 Autosampler. The peptides were loaded onto a self-packed biphasic C18/SCX MudPIT column using a Helium-pressurized cell (pressure bomb). The MudPIT column consisted of 360 μm x 150 μm i.d. fused silica, fritted with a filter-end fitting (IDEX Health & Science), and packed with 5cm of Luna SCX material (5 μm bead, Phenomenex) and 4 cm of Jupiter C18 material (5 μm bead, Phenomenex). After sample loading, the MudPIT column was connected using an M-520 microfilter union (IDEX Health & Science) to an analytical column (360 μm x 100 μm i.d.), equipped with a laser-pulled emitter tip. The analytical column was packed with 20cm Jupiter C18 material (3 μm bead, Phenomenex. Using the Eksigent NanoLC and Autosampler, MudPIT analysis was performed with an 8-step salt pulse gradient (0 mM, 50 mM, 100 mM, 150 mM, 200 mM, 300 mM, 500 mM, and 1 M ammonium acetate). Peptides were eluted from the analytical column after each salt pulse with a 105 min reverse gradient (2-40% acetonitrile, 0.1% formic) for the first 7 salt pulses, and a 2-95% acetonitrile for the last salt pulse. Gradient-eluted peptides were introduced into the mass spectrometer via nanoelectrospray ionization.

Data were collected using a 17-scan event, data-dependent method. Full scan (m/z 350-2000) were acquired with the Orbitrap as the mass analyzer (resolution 60,000), and the 16 most abundant ions in each MS scan were selected for fragmentation in the LTQ Velos. An isolation width of 2 m/z, an activation time of 10 ms, and 35% normalized collision energy, a maximum injection time of 100 ms and an AGC target of $1x10^4$ were used to generate MS/MS spectra. Dynamic exclusion was enabled, using a repeat count of 1, repeat duration of 10 sec, and an exclusion duration of 30sec.

For identification of acetylated peptides, raw data were extracted using ScanSifter and searched with SEQUEST (Thermo Fisher Scientific) against a *Rattus norvegicus* subset database created from the Uniprot KB protein database (www.uniprot.org). The protein database was a concatenated forward and reversed (decoy) database. Searches were configured to use variable modification of +57.0214 on Cys (carbamidomethylation), +15.9949 on Met (oxidation), and +42.0.056 on Lys (acetylation). Search results were assembled using Scaffold 3.0 (Proteome Software), where data were filtered to a protein and peptide threshold of 2% and 0.5% FDR respectively. Acetylated peptides of interest were validated via manual interrogation of the raw tandem mass spectra.

Immunoprecipitation and Western Blotting

For p75NTR western blot, whole cell lysates from mCherry-p75NTR-GFP (wildtype or mutant) overexpressing Hek 293 cells were prepared in NP-40 lysis buffer (25 mM Tris (pH 7.4), 137 mM NaCl, 2.7 mM KCl, 1% Nonidet P-40, and 10% glycerol) supplemented with a Complete Mini EDTA-free protease inhibitor mixture tablet (Roche) and a PhosStop phosphatase inhibitor mixture tablet (Roche). Cell lysates were subjected to SDS-PAGE and western blot analysis using antibody against p75NTR ICD (1:1000).

For HDAC1 immunoblotting, primary neurons were cultured in cell culture inserts and axons were lysed in NP-40 lysis buffer (25 mM Tris (pH 7.4), 137 mM NaCl, 2.7 mM KCl, 1% Nonidet P-40, and 10% glycerol) supplemented with a Complete Mini EDTA-free protease inhibitor mixture tablet (Roche) and a PhosStop phosphatase inhibitor mixture tablet (Roche). Cell lysates were subjected to SDS-PAGE and Western blot analysis using antibodies against HDAC1 (1:2000, Millipore), Histone H3 (1:3000, Abcam), Tau (1:1000, Cell signaling technology).

For immunoprecipitation, neurons were grown in mass cultures as described above and treated as indicated in figure legends. After treatment, neurons were collected and suspended in Buffer A (10 mM HEPES, 1.5 mM $MgCl_2$, 10 mM KCl, 0.5 mM DTT and Complete Mini EDTA-free protease inhibitor mixture), then lysed in glass homogenizer. The nuclei were pelleted by centrifugation at 750xg for 5 min, then the supernatant was collected and centrifuged again to remove any remaining nuclei. The supernatant was considered the cytosolic fraction and was treated with a detergent solution to solubilize cytosolic proteins in RIPA buffer (150 mM NaCl, 50 mM Tris (pH 7.5), 1% NP-40, 0.5% deoxycholate, and Complete Mini EDTA-free protease inhibitor mixture). Transfected HEK293 cells were processed similarly to make cytosolic fractions and analyzed by immunoprecipitation and western blotting with the indicated antibodies.

The cytosolic solutions were immunoprecipitated with anti-acetyl lysine agarose beads (25 ul beads per mg of protein), anti-dynein intermediate chain antibody (1ul per 100 ug protein), anti-$p150^{Glued}$ antibody (1ul per 100 ug protein) or anti-myc antibody (1:1000) as indicated in figure legends. Western blotting was done using following antibodies as indicated: anti- $p150^{Glued}$ antibody (1:1000), anti-myc (1: 1000), anti-tubulin (1:1000) or anti-dynein intermediate chain antibody (1: 1000).

QUANTIFICATION AND STATISTICAL ANALYSIS

Statistical Analyses

Number of experiments and sample sizes were as indicated in the figure legends. Data were collected randomly. Counts for analyzing neuronal apoptosis, p75NTR cleavage in distal axons and p75NTR co-localization with CD63 was done in a blinded manner such that the investigator was not aware of the treatment while counting. All graphs and statistical analyses were done using GraphPad Prism software. Student's t tests were performed assuming Gaussian distribution as indicated. One-way or two-way ANOVA analyses were performed when more than two groups were compared. Statistical analyses were based on at least 3 independent experiments, and described in the figure legends. All error bars represent the standard error of the mean (s.e.m).